SCIENCE CHINA PRESS

SCIENCE CHINA Life Sciences
life.scichina.com link.springer.com
https://doi.org/10.1007/s11427-024-2904-6

RESEARCH PAPER

Population genomic landscapes and insights for conservation of the critically endangered island-endemic Chinese pangolin in Taiwan

Tianya Zhai[1], Jichao Wang[2], Guangquan Zhan[3], Jingyang Hu[1*] & Li Yu[1,4*]

[1]State Key Laboratory for Conservation and Utilization of Bio-Resources in Yunnan, Yunnan University, Kunming 650091, China
[2]Ministry of Education Key Laboratory for Ecology of Tropical Islands, Key Laboratory of Tropical Animal and Plant Ecology of Hainan Province, College of Life Sciences, Hainan Normal University, Haikou 571158, China
[3]Veterinary Hospital, Ningbo Zoo, Ningbo 315042, China
[4]Southwest United Graduate School, Kunming 650091, China

*Corresponding authors (Li Yu, email: yuli@ynu.edu.cn; Jing Yang Hu, email: hujingyang@ynu.edu.cn)

Received 21 December 2024; Accepted 11 March 2025; Published online 11 July 2025

Island species/populations are characterized by evolutionary uniqueness and a high degree of endemism and extinction. The conservation and restoration of island species/populations have become the most challenging and urgent issues in biodiversity conservation. Chinese pangolin in Taiwan island (*Manis pentadactyla pentadactyla*) is a well-known, critically endangered, and island-endemic Chinese pangolin subspecies, which has been the focus of conservation concern. Here, we first generated large-scale population genomics data for the Chinese pangolin in Taiwan to address its population structure, demographic history, the genomic consequences of population declines, and survival potential. We revealed that the Chinese pangolin in Taiwan originated in southeast China and was differentiated into Northern and non-Northern populations due to the isolation of the Xueshan and Central Mountain Ranges, proposing to treat them as separate conservation units. The southeast of Taiwan island acted as a refuge for this Chinese pangolin subspecies during the Last Glacial Maximum. The Northern population had experienced a more severe bottleneck and isolation than the non-Northern population, which corresponded to the estimated current lower genetic diversity, higher inbreeding, and genetic load of the Northern population. The modeling results revealed that the Northern population is more seriously affected by climate change than the non-Northern population, which highlights that climate change poses a substantial threat to island biodiversity. The simulation results indicate that the Northern population needs a higher population growth rate to achieve evolutionary potential equal to the non-Northern population over the next 100 years, deserving conservation prioritization. This study enhances the understanding of genetic background, conservation status, and future prospects for Chinese pangolin in Taiwan, as well as the genetic consequences of a small and isolated island population.

pangolins | island population | population genomics | conservation genomics

INTRODUCTION

The current rate of species extinction is hundreds or even thousands of times faster than in the past, and it has been reported that life on Earth is facing the sixth mass extinction (Butchart et al., 2010; Ceballos et al., 2015; Ceballos et al., 2017; Pimm et al., 2014). Notably, since the 1500 Common Era (CE), over 60% of terrestrial extinctions have occurred on islands (http://www.iucnredlist.org), and this has exerted a substantial and profound impact on the global ecosystem (Matthews et al., 2021; Tershy et al., 2015). This is due to the fact that island species/populations are characterized by a limited distribution area, habitat frangibility, and small population size. They are, therefore, more vulnerable to environmental change and are more likely to suffer a loss of genetic diversity, thus reducing the fitness of individuals and increasing the extinction risk of species (Crooks et al., 2017; Mayr, 2013; Schrader et al., 2024). Meanwhile, factors driven by human activities, such as illegal hunting and trade (Holdaway and Jacomb, 2000; Mack and Wright, 1998), habitat degradation (Maunder et al., 1999), and the introduction of invasive alien species (Cooke et al., 2017), are exacerbating the threats to the survival of vulnerable island populations. The conservation and restoration of island populations have become the most challenging and urgent issues in biodiversity conservation (Heinen et al., 2018; Kier et al., 2009; Whittaker et al., 2017).

Chinese pangolin in Taiwan island (*Manis pentadactyla pentadactyla* Linnaeus, 1758), a well-known Taiwan island-endemic Chinese pangolin subspecies (Allen, 1938; Ellerman and Morrison-Scott, 1951; Sun et al., 2021; Wu et al., 2007), exists as a small and isolated population (Wilson and Reeder, 2005), which has been classified as critically endangered on the red list

Citation: Zhai, T., Wang, J., Zhan, G., Hu, J., and Yu, L. (2025). Population genomic landscapes and insights for conservation of the critically endangered island-endemic Chinese pangolin in Taiwan. Sci China Life Sci 68, 2768–2783. https://doi.org/10.1007/s11427-024-2904-6

CrossMark click for updates

of the International Union for Conservation of Nature (IUCN) (http://www.iucnredlist.org). In the 1950s and 1960s, at least 60,000 Chinese pangolins in Taiwan were killed annually for the international leather trade, which caused the population size to suffer a severe decrease (Challender et al., 2015; Chao, 1989; Willcox et al., 2019). Although the Wildlife Conservation Act has been in place since 1989 and the Chinese pangolin in Taiwan has recovered to approximately 15,000 individuals in recent times (Kao et al., 2020), their evolutionary uniqueness and high degree of endemism and extinction risk make this Chinese pangolin subspecies in need of urgent conservation action.

Investigating the population structure, the demographic history, and the genomic consequences of population declines, as well as survival potential, can provide critical insights into a species'/population's genetic background and conservation status, thereby facilitating strategic conservation planning (Buckland et al., 2014; Frankham et al., 2002; Funk et al., 2012; Hohenlohe et al., 2021). Based on the mitochondrial gene and microsatellite markers, two (northern and central-southern) to four (northern, central, southern, and eastern) genetic populations in this Chinese pangolin subspecies (Liu, 2017; Wang, 2007) have been found, which has been controversial. The demographic history and survival potential analyses based on one genome indicated that this Chinese pangolin subspecies arrived on Taiwan island via land bridge around 10,000 years ago (Hu et al., 2020; Wei et al., 2024) and has lower survival potential compared with Chinese pangolin in the Chinese mainland (Hu et al., 2020). The low survival potential of Chinese pangolin in Taiwan was also supported by the population microsatellite marker analyses (Sun et al., 2020). However, all of these studies are based on the analyses of either only one genome (Choo et al., 2016; Houck et al., 2023; Hu et al., 2020; Wei et al., 2024) or short gene fragments (Liu, 2017; Sun et al., 2020; Wang, 2007). Population genomic analysis is thus essential for systematically and comprehensively addressing these issues, thereby promoting the development of effective conservation strategies for the Chinese pangolin in Taiwan.

In this study, we generated, for the first time, population genomics data for Chinese pangolin in Taiwan covering the northern, central, southern, and eastern parts of Taiwan island. Our population genomic study enhanced the understanding of the genetic background, conservation status, and future prospects of this Chinese pangolin subspecies. This study provides valuable information concerning the genetic impact of population size declines and conservation insights into this critically endangered island-endemic population.

RESULTS

Population genomic dataset

Whole genome resequencing was conducted on 35 Chinese pangolins, including 33 Chinese pangolins in Taiwan (Figure 1A) and two Chinese pangolins in non-Taiwan island (Table S1), yielding an average mapping depth of 10.71-fold (7.77-fold to 25.18-fold) and an average mapping rate of 99.79% (99.50% to 99.90%) (Table S2). Concurrently, we downloaded the published resequencing data for 95 Chinese pangolins, including two Chinese pangolins in Taiwan and 93 Chinese pangolins in non-Taiwan island, with an average mapping depth of 17.75-fold (5.93-fold to 39.67-fold) and an average mapping rate of 98.88% (93.70% to 99.79%) (Table S2). Finally, we constructed a dataset encompassing a total of 130 Chinese pangolins, including 35 Chinese pangolins in Taiwan and 95 Chinese pangolins in non-Taiwan island, in order to investigate the phylogenetic relationship between population in Taiwan and other Chinese pangolin populations. We also constructed a separate dataset of 35 Chinese pangolins in Taiwan specifically to study their population structure, demographic history, and evolutionary potential. The SNP calling and filtering produced a total of 13,865,554 and 3,010,865 bp high-quality autosomal SNPs for the two datasets, respectively.

Population structure

Based on the dataset of 130 Chinese pangolins, we explored the relationship between Chinese pangolin in Taiwan and other Chinese pangolin populations. Phylogenetic analyses strongly support the idea that the Chinese pangolin is divided into five genetic populations, among which the subspecies in Taiwan is a monophyletic genetic population (Figure 1B). Admixture analyses (Figures S1 and S2) and principal component analyses (PCA) (Figure S3) also support the idea that the subspecies in Taiwan is an independent genetic component. Furthermore, phylogenetic analyses showed that the subspecies in Taiwan diverged from the southern China population (MPB2) and had the closest relationship with individuals from Zhejiang, Anhui, Jiangxi, and Fujian (Figure 1B; Table S2). These individuals also showed admixture signals with individuals in Taiwan in admixture analyses and had the greatest similarities with individuals in Taiwan in PCA (Figures S1 and S3). These results suggest that the Chinese pangolin in Taiwan originated from southeastern China.

Phylogenetic analyses supported that Chinese pangolin in the four geographic parts (northern, central, southern, and eastern parts of Taiwan island) of Taiwan was divided into two main distinct populations, i.e., the Northern (the individuals from northern Taiwan island) and the non-Northern populations (the individuals from central, southern, and eastern Taiwan island) (Figure 1C). The admixture analyses and PCA also confirmed the separation of the Northern and non-Northern populations by the lowest cross-validation (CV) error when K=2 (Figure S4) on the basis of the first PCA component (PC1) (Tracy-Widom, P value<0.001) (Figure 1D and E). The Weir and Cockerham weighted F_{ST} value and the genetic distance between Northern and non-Northern populations were 0.16 and 0.21, respectively (Figure S5), which further indicated large genetic differentiation between these two populations. EEMS analysis also reflected a significant differentiation barrier located in the Xueshan Mountain Range and Central Mountain Range between Northern and non-Northern populations (Figure 1F), suggesting that the mountain barrier may be responsible for the genetic differentiation of Chinese pangolin in Taiwan.

In addition, admixture analyses and PCA revealed three subgroups within the non-Northern population, corresponding to central, southern, and eastern geographic parts of Taiwan island when K=4 and in the context of the second PCA component (PC2) (Tracy-Widom, P value<0.001), which was consistent with the clustering of three subgroups in the phylogenetic analyses (Figure 1C–E). The Weir and Cockerham weighted F_{ST} value and genetic distance between these three subgroups were in the ranges of 0.09–0.13 and 0.18–0.20,

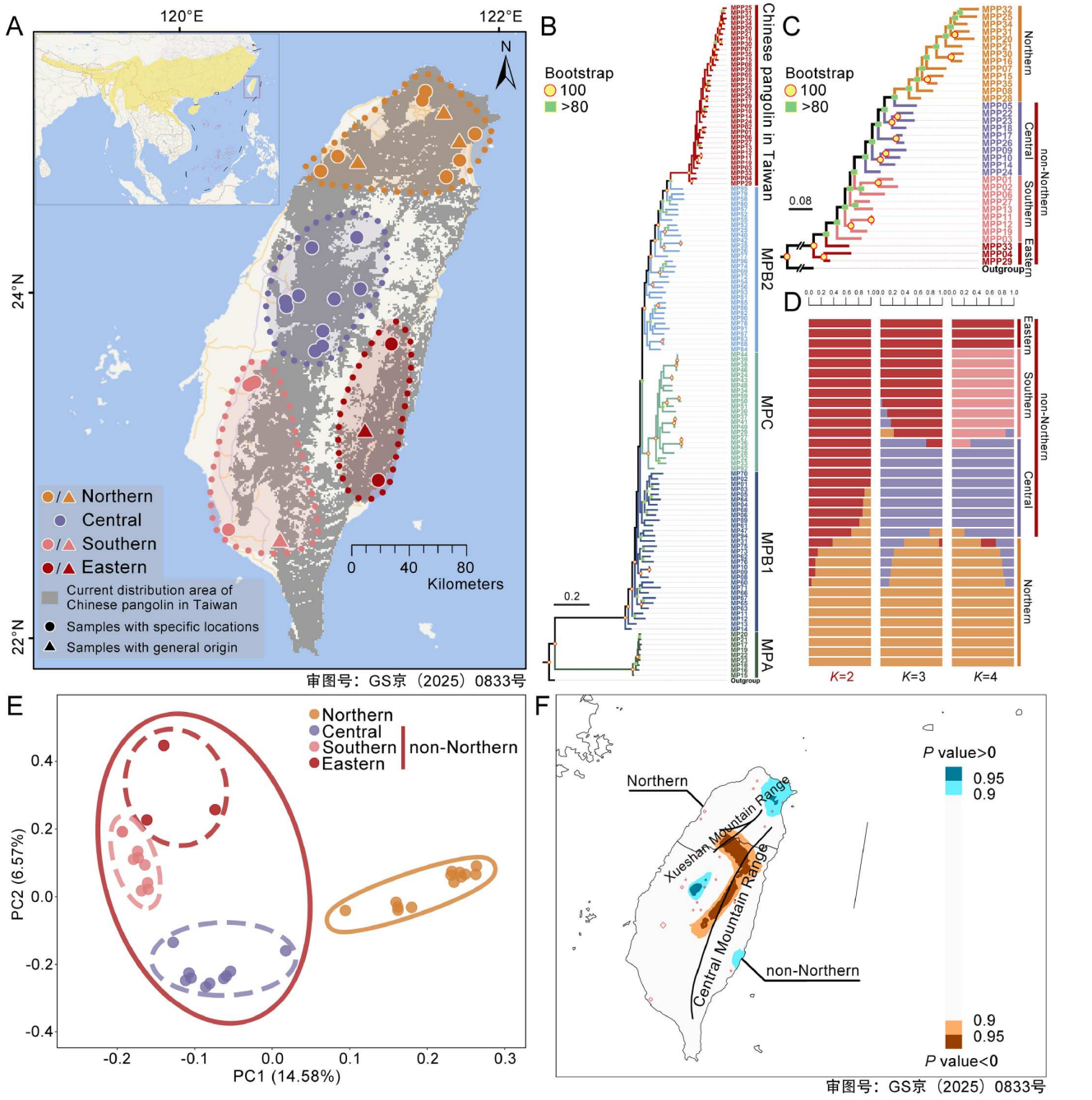

Figure 1. Sample collection and population structures of Chinese pangolin and subspecies in Taiwan. A, Distribution range and sampling locations of the subspecies in Taiwan. The distribution of the Chinese pangolin is shown in the upper left corner and is indicated in yellow (Challender et al., 2019). Current distribution range of the subspecies in Taiwan is shaded gray (Chang et al., 2022). Major geographic lineages in the subspecies in Taiwan are indicated as follows: northern (orange), central (purple), southern (pink), eastern (red) (Wang, 2007). B, ML phylogenetic tree of Chinese pangolin. MPA, MPB1, MPB2, and MPC represent the four genetic populations of Chinese pangolin in non-Taiwan island, which correspond to those from Wei et al. (2024). Nodes with bootstrap support >80% are shown. C, ML phylogenetic tree of Chinese pangolin in Taiwan. Nodes with bootstrap support >80% are shown. D, Admixture analysis of Chinese pangolin in Taiwan. The optimal *K* value was set to 2 (Figure S4). E, Principal component analysis (PCA) for Chinese pangolin in Taiwan. F, Model of effective migration rates of Chinese pangolin in Taiwan. Brown, areas of significantly low migration relative to the average; blue, areas of significantly higher migration.

respectively, indicating moderate degrees of genetic differentiation (Figure S5) and supporting the possible existence of subpopulations within the non-Northern population.

Genetic diversity, inbreeding level, and genetic load

The average genetic diversity (heterozygosity, He) and inbreeding coefficient (F_{ROH}>100 kb) for all Chinese pangolins in Taiwan were 0.029% and 44.3%, respectively (Figure 2A and B; Table S3). The Northern population had significantly lower genetic diversity and a significantly higher inbreeding coefficient, i.e., more serious inbreeding, than the non-Northern population (0.027% *vs.* 0.031%, Wilcoxon rank-sum test, *P* value<0.05; 48.4% *vs.* 41.9%, Wilcoxon rank-sum test, *P* value<0.05)

https://doi.org/10.1007/s11427-024-2904-6

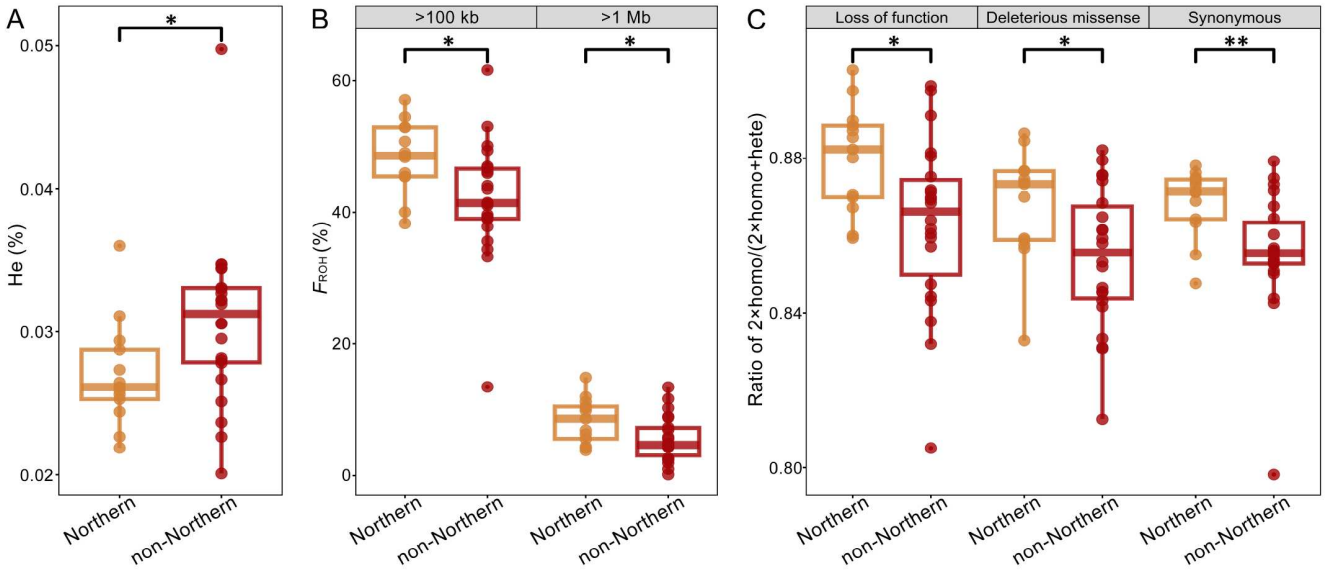

Figure 2. The current evolutionary potential of Chinese pangolin in Taiwan. (A) Heterozygosity, (B) inbreeding coefficient, and (C) genetic load for the Northern and non-Northern populations of Chinese pangolin in Taiwan, * P<0.05; ** P<0.01.

(Figure 2A and B; Table S3). In addition, the genetic load of functional loss mutations, deleterious missense mutations, and synonymous mutations for the Northern population were all at significantly higher levels than for the non-Northern population (0.88 *vs.* 0.86, Wilcoxon rank-sum test, P value<0.05; 0.88 *vs.* 0.85, Wilcoxon rank-sum test, P value<0.05; 0.87 *vs.* 0.86, Wilcoxon rank-sum test, P value<0.01, respectively) (Figure 2C; Table S3). These results indicated the lower current evolutionary potential of the Northern population than that of the non-Northern population.

Demographic history and historical ecological niche simulation

We inferred the demographic histories (Figure 3A and B) and simulated the historical ecological niche changes of Chinese pangolin in Taiwan (Figure 3C and D). The demographic history inference showed that the Chinese pangolin in Taiwan first experienced a population expansion about 8.61 (8.49–8.73) thousand years ago (kya), which may have been associated with the temperature increasing during the early Holocene (11.70–8.20 kya) (Antevs, 1953; Walker et al., 2012). The Northern population diverged from the non-Northern population at 6.40 kya (Figure 3A), corresponding to the warmest period (7.70–6.00 kya) of the Mid Holocene (MH) (Antevs, 1953; Kaufman and Broadman, 2023). Interestingly, the historical ecological niche modeling also suggested that the warmer climate during the Mid Holocene led to the suitable habitat emergence and expansion in the Northern population, compared with the limited distribution of suitable habitat in the southeast of Taiwan island during the Last Glacial Maximum (LGM; 22.00 kya) (Berends et al., 2021; Bintanja et al., 2005) (Figure 3C and D). This would have promoted the divergence of the Northern population from the non-Northern population. Moreover, for the non-Northern population, there were significantly higher outgroup *f3* values (Figure 4A; Table S4), significantly more shared haplotypes with the ancestor population (Figure 4B), more private variants (Figure 4C), and a faster speed of decline for the linkage disequilibrium (Figure 4D) than for the Northern population, further confirming that the Northern population diverged from the non-Northern population. Intriguingly, the Northern/non-Northern population split occurred during the Neolithic (about 7.00–6.00 kya) (Qiu et al., 2023), when human activities increased and the development of production tools drove the exploitation of the plains and hilly areas, with the Northern population being the most affected (Cruz Berrocal et al., 2018; Zang, 1998). This may have interrupted migration routes and promoted the divergence of the two populations of Chinese pangolin in Taiwan.

After the split, both the Northern and non-Northern populations experienced an abrupt decline 49 and 63 years ago, respectively (Figure 3A), with the effective population size (*Ne*) decreasing by a factor of approximately 103 (from about 5,881 to 57 individuals) and 45 (from about 10,941 to 243 individuals). The *Ne* of the Northern population was found to be significantly smaller than that of the non-Northern population, indicating that the Northern population experienced a stronger population bottleneck, which may be associated with the population history dynamics and the environmental adaptability. In addition, the frequency of gene flow between these two populations significantly decreased after the population decline (Figure 3A). Moreover, the intensity of gene flow output from the Northern population has always been higher than the input from the non-Northern population, and the intensity has been stronger since the population decline, which is consistent with the observed smaller size of the Northern population. Besides the significant declines of the two populations in recent decades and the steeper decline in the Northern population, the reconstruction of the demographic history of the past 10 years (Figure 3B) revealed that the *Ne* of the Northern population remained very small, while the non-Northern population slightly increased (at a rate of about 5%), again indicating that the Northern population is a smaller population than the non-Northern population, while the non-Northern population may be benefiting more from

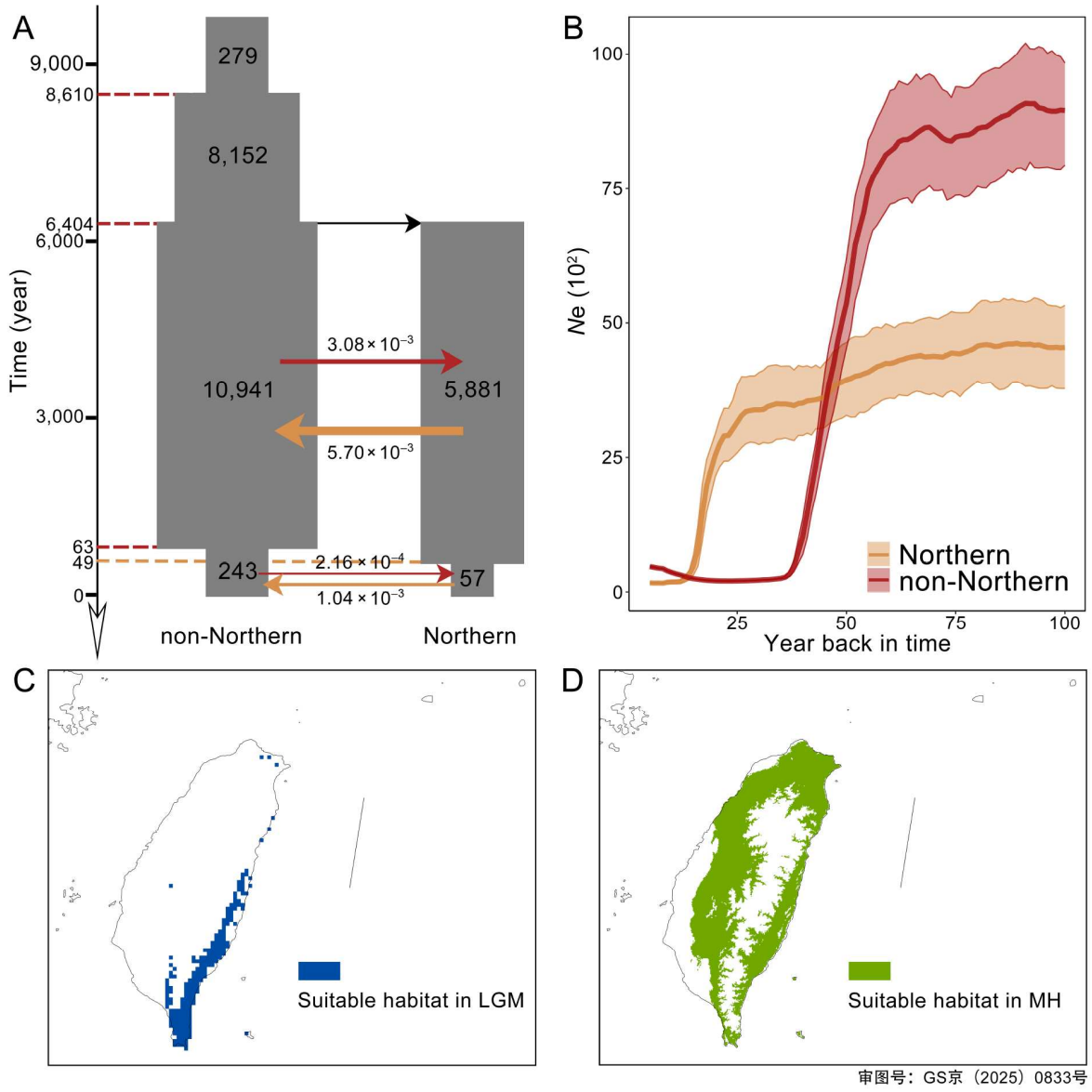

Figure 3. Demographic history and historical ecological niche simulation of Chinese pangolin in Taiwan. A, The demographic history of Chinese pangolin in Taiwan. The figure on the node indicates the time of historical events, and the number of migrants per year between populations is shown next to the colored arrow. B, The recent demographic history of Chinese pangolin in Taiwan. The thick lines represent the average effective population sizes (Ne) over the past 100 years, and the light shaded regions represent the 95% confidence intervals. C, The suitable habitat for Chinese pangolin in Taiwan during the LGM. D, The suitable habitat for Chinese pangolin in Taiwan in the MH.

recent conservation efforts. Interestingly, the recent ecological observation based on long-term field monitoring records showed that the population size of the Northern population remained constant, while the non-Northern population increased quickly in recent years (Weng et al., 2023), which further supported our results.

Future ecological niche and local genetic offset modeling

We performed future ecological niche modeling and local genetic offset modeling to predict the changes in suitable habitats and local climate adaptation of Chinese pangolin in Taiwan in the future from 2081 to 2100 under an optimistic scenario of greenhouse effect with an average annual temperature increase of 0.5–1.5°C (Shared Socioeconomic Pathway, SSP 1-2.6) and a worst-case scenario with an average annual temperature increase of 2.4–4.8°C (SSP5-8.5). Under the SSP1-2.6 scenario, the suitable habitat area for the Northern population was predicted to decrease by 9.30% compared with the current area, while that for the non-Northern population will increase by 4.68% (Figure 5A and B). Under the SSP5-8.5 scenario, the decrease in suitable habitat area for the Northern population is much greater, up to 58.57%, and the suitable habitat area for the non-Northern population showed a decrease of 8.74% (Figure 5A and C). These findings indicate that under the risk of future climate warming, especially as the degree of greenhouse effect increases to the level of SSP5-8.5, the suitable habitat area of Northern and non-Northern populations will shrink, and the reduction in area will be more severe for the Northern population. Consistently, the local genetic offset analyses based

on 75 climate-associated SNPs (Table S5) suggested that the local genetic offset of these two populations under SSP5-8.5 would be higher than that under SSP1-2.6 (Figure 5D and E, 61.24% and 41.95% higher for the Northern and non-Northern populations, respectively), indicating that the suitable habitat under SSP5-8.5 will be smaller than that under SSP1-2.6 and that the predicted scenario under SSP5-8.5 will have a more severe impact on the survival of Chinese pangolin in Taiwan. Simultaneously, in both scenarios, the genetic offset observed in the Northern population was significantly higher than that in the non-Northern population (3.09×10^{-2} *vs.* 1.99×10^{-2} under SSP1-2.6, Wilcoxon rank sum test, P value<0.001; 4.98×10^{-2} *vs.* 2.85×10^{-2} under SSP5-8.5, Wilcoxon rank sum test, P value<0.001), suggesting that the Northern population has less potential to adapt to the new local climate conditions and will be more adversely impacted by climate change in the future than the non-Northern population.

In addition, as the climate warms in the future, suitable habitats for both populations will change in order to respond to the new conditions. For the Northern population, the center of the suitable habitat will move 8.70 and 12.18 km southeast from Taoyuan to New Taipei, northern Taiwan island, in the case of SSP1-2.6 and SSP5-8.5, respectively (Figure 5B and C). For the non-Northern population, the center of the suitable habitat will move 21.75 and 60.48 km north from Kaohsiung to Nantou, central Taiwan island, in the case of SSP1-2.6 and SSP5-8.5, respectively (Figure 5B and C). The distance of this move for the Northern population is significantly shorter than that for the non-Northern population, indicating that the area suitable for the Northern population is narrower and more vulnerable. The changes to the centers of suitable habitat provide a scientific basis for determining the future key habitats for these two populations and formulating targeted conservation measures.

Evolutionary potential simulation

We evaluated the future evolutionary potential by calculating the number of deleterious mutations, heterozygosity, inbreeding level, and fitness of the populations over the next 100 years based on their current population sizes (Figure 6A–H). The results showed that there was no significant difference in the clearance of strong and moderately deleterious mutations between the two populations (Figure 6B and C), while the accumulation of weak deleterious mutations was significantly higher in the Northern than the non-Northern population (Wilcoxon rank sum test, P value<0.01) (Figure 6D). Concurrently, compared with the non-Northern population, the Northern population had significantly more fixed deleterious mutations (Wilcoxon rank sum test, P value<0.001) (Figure 6E), decreased heterozygosity, an increased inbreeding coefficient and decreased fitness (Wilcoxon rank sum test, P value<0.001) (Figure 6F–H). These findings suggest that the Northern population will have lower evolutionary potential than the non-Northern one over the next 100 years if a constant population size is maintained.

We also considered the future evolutionary potential of the populations under different population growth rates (1%, 3%, 5%, and 7%). For both populations, the three kinds of deleterious mutations (strong, moderate, and weak) exhibited the same change trend across different growth rates (Figure 6I–K), and the heterozygosity was not predicted to decline and will maintain a stable state when the growth rates reach 3% (Figure 6M). Notably, fixed deleterious mutations and the inbreeding coefficient were not predicted to continue to increase when the growth rate reached 3% for the Northern population, while the growth rate reached 1% for the non-Northern population in the same case (Figure 6L and N). This indicates that the Northern population will need a higher population growth rate to prevent fixed deleterious mutations and inbreeding from increasing in the future. Consistently, when the growth rate was 1%, 3%, 5%, and 7%, the fitness of non-Northern population was found to return to 92.50%, 95.32%, 96.34% and 97.10% of the pre-bottlenecked level, while that of Northern population was only able to return to 89.90%, 94.46%, 95.63% and 96.69% of the pre-bottlenecked level (Figure 6O), again suggesting that the Northern population needs a higher population growth rate to achieve the same level of future population recovery as the non-Northern population.

DISCUSSION

In this study, we generated, for the first time, population genomics data for Chinese pangolin in Taiwan covering the northern, central, southern, and eastern parts of Taiwan island. This allowed us to examine the population structure, demographic history, and genomic consequences of population declines as well as the survival potential, with enhanced understanding of the genetic background, conservation status, and future prospects for Chinese pangolin in Taiwan. This study provides valuable information concerning the genetic impact of population size declines and conservation insights into this critically endangered island-endemic population.

Our research identified the Chinese pangolin in Taiwan as a separate population that originated in southeast China and most likely in Zhejiang, Anhui, Jiangxi, and Fujian, thus pinpointing the origin of this subspecies in Taiwan from the previously known southeastern China region (Hu et al., 2020) more precisely. Furthermore, the current subspecies in Taiwan are divided into Northern and non-Northern genetic populations due to the isolation by the Xueshan and Central Mountain Ranges, thus establishing the need to treat them as separate conservation units in the conservation and management. This genetic division is consistent with the results based on microsatellite marker analyses, which reveal that Chinese pangolin in Taiwan is divided into central-southern and northern populations (Liu, 2017) and does not support the proposal of four populations (northern, central, southern and eastern populations) based on mitochondrial gene analyses (Wang, 2007). Intriguingly, the Xueshan Mountain Range and Central Mountain Range, which separate the Northern and non-Northern genetic populations, have previously been suggested as the main cause for the differentiation of endemic animals in Taiwan distributed on the north and south sides of the mountains. Examples include wood mouse in Taiwan, which has been characterized by two divergent populations in the northern and south-central regions (Hsu et al., 2001), and Taipei treefrog, which exhibits two genetic lineages in the northern and central areas (Yang et al., 1994). It is noteworthy that the Central Mountain Range has also been reported to have been responsible for the differentiation of the small-endemic animals in Taiwan distributed on the western and eastern sides, such as the Indian rice frog and gossamer-wing damselfly (Huang and Lin, 2011; Toda et al., 1998), due to their weak migration ability. However, the western-eastern population structure is not apparent in Chinese pangolin in Taiwan, suggesting that the Central Mountain Range alone is not as

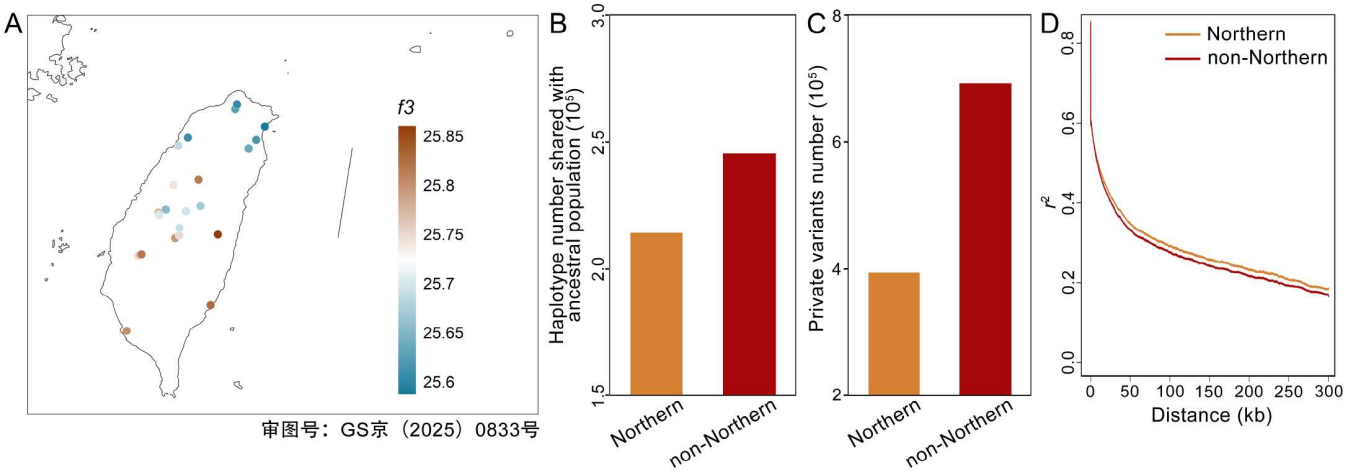

Figure 4. The outgroup *f3* statistic, haplotype sharing analysis, private variants, and LD decay rate of Chinese pangolin in Taiwan. A, Outgroup *f3* statistic between each individual of Chinese pangolin in Taiwan and the ancestral population; the higher the outgroup *f3* value, the closer the genetic relatedness. B–D, (B) Number of haplotypes, (C) number of private variants, and (D) linkage disequilibrium (LD) for the Northern and non-Northern populations of Chinese pangolin in Taiwan.

strong a barrier for Chinese pangolin in Taiwan as it is for small-endemic animals in Taiwan. In addition, we also found a moderate degree of differentiation between individuals from the central, eastern, and southern parts of Taiwan island within the non-Northern population, which provides genomic evidence to support the suggestion that the terrain, rivers, roads, and the Coastal Mountain Range have a certain barrier effect on the gene flow within non-Northern population (Wang, 2007).

Our historical ecological niche simulation suggested that the southeast of Taiwan island acted as a refuge for Chinese pangolin in Taiwan during the Last Glacial Maximum. Interestingly, studies of many other endemic Taiwan species, such as the red-bellied tree squirrel, ring cupped oak, long leaf evergreen chinkapin, and Gokkohu yungai, have also suggested that the southeast of Taiwan island was their refuge during this period (Chen et al., 2017a; Cheng et al., 2005; Huang et al., 2002; Oshida et al., 2006). These results show that many species on Taiwan island exhibited similar survival strategies to overcome the cold climate of the Last Glacial Maximum. In addition, the results of demographic history and historical ecological niche simulation revealed that, after the end of the Last Glacial Maximum, the warmer climate promoted the expansion of Chinese pangolin in Taiwan and the divergence of the Northern population from the non-Northern population, a similar pattern observed in other endemic species in Taiwan, such as sambar deer, torrent carp, and oriental river prawn (Chen et al., 2017b; Ju et al., 2018; Li et al., 2023). Our study represents an example of how climate change plays an important role in patterns of genetic division for Chinese pangolin in Taiwan, which are temperature-sensitive medium-sized mammals (Challender et al., 2020).

Our recent demographic reconstruction shows that the Northern population has experienced a more severe population bottleneck and greater isolation compared with the non-Northern population, which can explain why the Northern population has lower current evolutionary potential. The effective population size has not recovered recently in the Northern population, which suggests that the restoration of an effective population size is a big challenge. The results of the ecological niche and local genetic offset modeling show that the Northern population is more vulnerable to future climate changes compared with the non-Northern population. In addition, evolutionary potential simulation indicates that the Northern population has lower evolutionary potential than the non-Northern one over the next 100 years. These results suggest that the Northern population is at greater risk of extinction and that the restoration of the effective population size for the Northern population should be a priority for future conservation. In contrast, the non-Northern population now has a larger effective population size than the Northern population. Consistently, the current estimated population size of the non-Northern population (11,580 individuals) has been reported to be larger than that of the Northern population (3,202 individuals) (Kao et al., 2019), further confirming the higher current evolutionary potential of the non-Northern population. Interestingly, our results show that the current effective population growth rate of the non-Northern population has reached 5%, and the evolutionary potential of the non-Northern population can be effectively restored in the future. Our study is the first to evaluate the conservation status and future prospects of the two genetic populations of Chinese pangolin in Taiwan, which suggests that the Northern population should be the focus of future conservation efforts.

Previous studies based on interviews have indicated that the pangolin leather trade resulted in the over-exploitation of Chinese pangolin in Taiwan from 1950 to 1970 (Chao, 1989), however, no studies have reported the genetic consequences of this. Our study reveals that it led to a considerable decline in the effective population of Chinese pangolin in Taiwan and decreased gene flow between the Northern and non-Northern populations. Given that the current intensification of population isolation may be largely caused by human activities, we propose promoting the restoration of gene flow between the Northern and non-Northern populations through the construction of ecological corridors. A recent study of endangered Madagascar island lemurs shows that the widespread gene flow between species maintains their extraordinarily high genetic diversity (Orkin et al., 2025) and high survival potential. The studies of Isle Royale wolf (Robinson et al., 2019) and New Zealand kākāpō (Dussex et al., 2021), two island species of which underwent population declines and lacked gene flow between species, are severely deficient in genetic

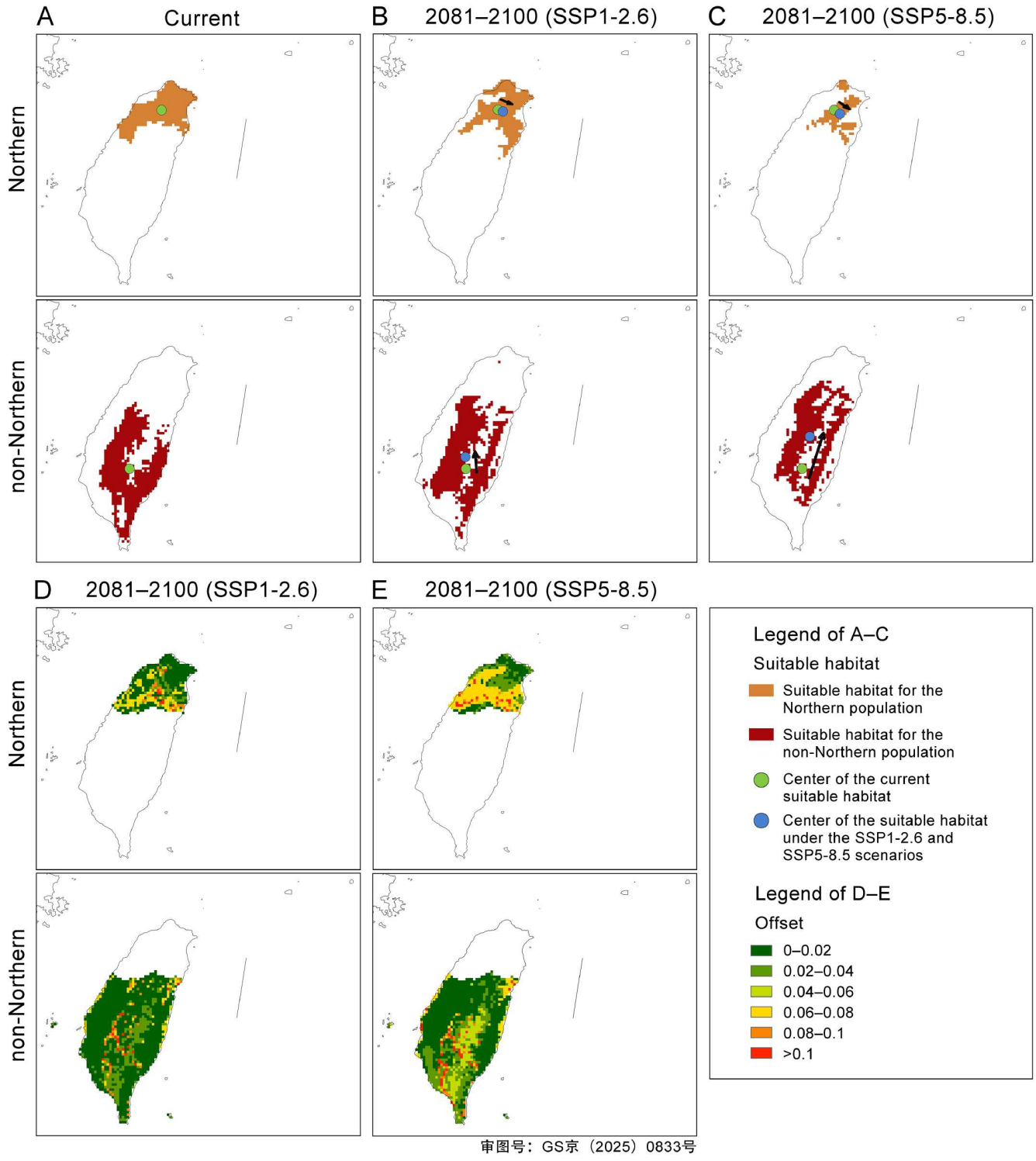

Figure 5. Future ecological niche modeling and local genetic offset modeling of Chinese pangolin in Taiwan. A–C, Ecological niche modeling for Northern and non-Northern populations. (A) Current suitable habitats, (B) suitable habitats under SSP1-2.6 in 2081–2100 and (C) suitable habitats under SSP5-8.5 in 2081–2100. The green and blue dots indicate the current and future center of the suitable habitats, respectively. D and E, Local genetic offset (GO) modeling for Northern and non-Northern populations. D, Genetic offsets under SSP1-2.6 in 2081–2100. E, Genetic offsets under SSP5-8.5 in 2081–2100. The higher the GO, the harder it is for individuals in the region to adapt to future climate.

diversity and survival potential, and thus have a high risk of extinction. Therefore, it is essential to restore gene flow between different populations to prevent further loss of genetic diversity and their capacity to adapt to changing environments.

Since the implementation of the Wildlife Conservation Act in 1989, the Chinese pangolin in Taiwan has been protected and

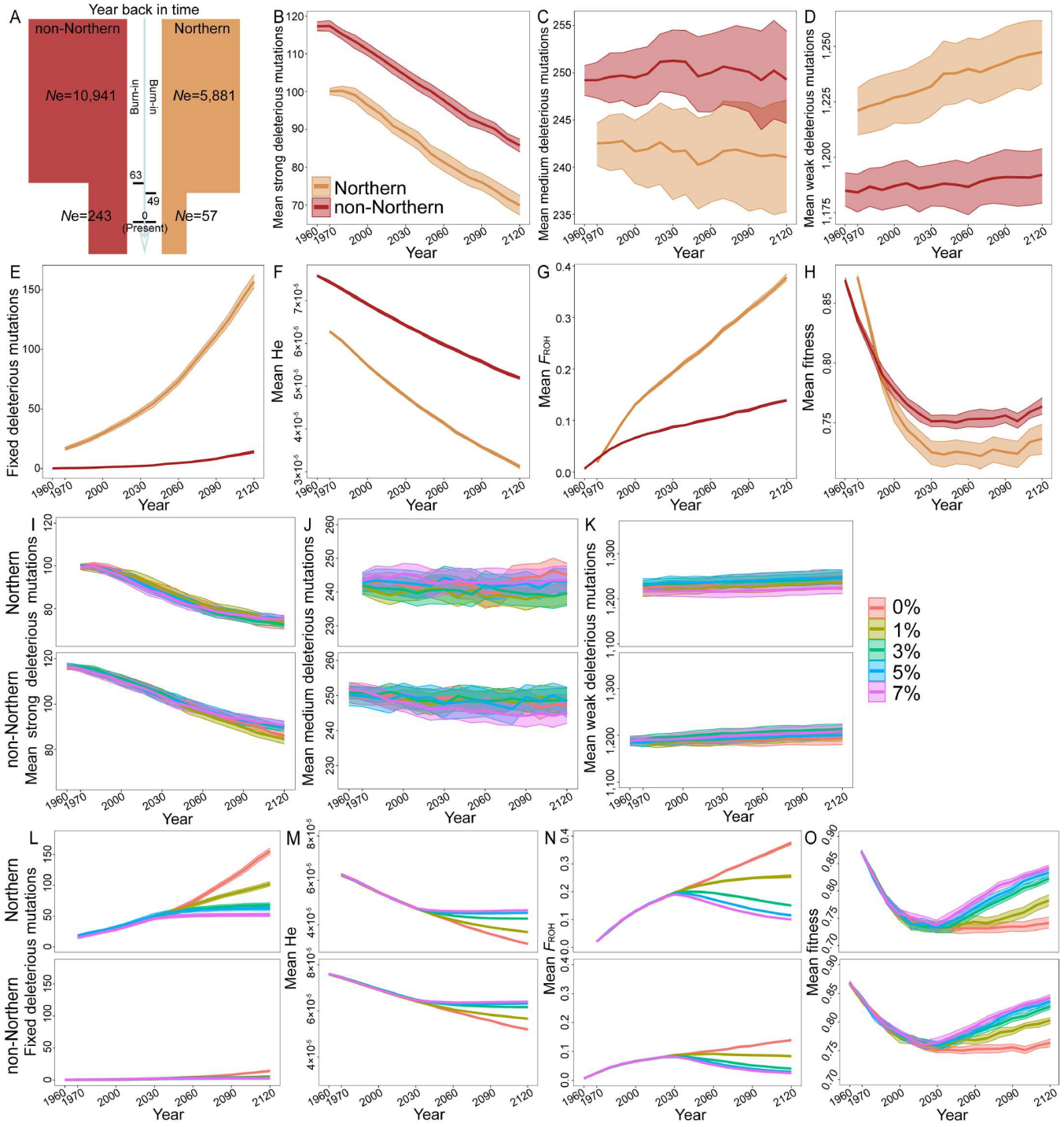

Figure 6. Simulation of the evolution potential for Chinese pangolin in Taiwan. A, The demographic history models used in simulations. B–H, The evolutionary potential under scenarios where Northern and non-Northern populations maintain their current small population size over the next 100 years. I–O, The evolutionary potential for Northern and non-Northern populations under different growth rates (0%, 1%, 3%, 5%, 7%) over the next 100 years.

recovered to approximately 15,000 individuals recently (Kao et al., 2020), making it the only recovering population, in stark contrast to the severe population declines reported in other pangolins around the world. However, the demographic history results indicate that the Northern population has not experienced a comparable recovery in effective population size as observed in the non-Northern population, and both the current and future evolutionary potentials of the Northern population are lower. Notably, even when population size is recovered in island species, the restoration of genetic diversity still needs attention. For instance, although the population of Channel Island fox has significantly rebounded from the bottleneck experienced in the 1990s, their genetic diversity did not recover, and they still struggle with the long-term environmental adaptation (Adams and Edmands, 2023; Robinson et al., 2018). Both Tiburon Island sheep (Hedrick et al., 2001) and Isle Royale moose (Kyriazis et al.,

https://doi.org/10.1007/s11427-024-2904-6

2023) have thrived over the past decade, but their genetic diversity is low and the inbreeding and genetic load levels increase, which could eventually threaten ultimate population viability. Therefore, long-term assessing and monitoring the genetic diversity in endangered island species is critical to provide information on their survival status and improve management of these populations that are less able to respond to novel challenges (Adams and Edmands, 2023). In view of this, we advocate for long-term monitoring of indicators such as genetic diversity in the Northern population, which will offer critical insights into their long-term survival and management. Simultaneously, we observed that climate warming would have more impact on the Northern population than the non-Northern population, given that they cannot adapt to future climate warming by migrating northward in the same manner as the non-Northern population. These results indicate that different island populations, akin to Northern and non-Northern populations of Chinese pangolin in Taiwan, are differentially affected by climate warming, and highlight the fact that greenhouse effect poses a substantial threat to biodiversity in different island populations (Leclerc et al., 2020; Manes et al., 2021; Waller et al., 2017). Due to the vulnerability of island species to climate change, we urge the international community to collaborate in addressing this global challenge by developing a circular carbon economy (including enhancing the efficiency of recycling waste materials, transition from fossil fuels to renewable energy sources) and enhancing public awareness of climate warming (van Daalen et al., 2024; Vidal et al., 2024).

MATERIALS AND METHODS

Sample collection

Thirty-three tissue samples of Chinese pangolin in Taiwan came from individuals that had died as a result of road accidents and had been taken to a rescue center. These samples represented 10 of 16 counties/cities covering their most geographic distribution area (Chang et al., 2022) and were provided by Taiwan University and Pingtung University of Science and Technology. These samples were classified into four geographic populations based on Wang (2007), including eleven northern, ten central, nine southern, and three eastern population individuals. We also downloaded the published genome resequencing data for two Chinese pangolins in Taiwan from Taipei Zoo (Choo et al., 2016; Houck et al., 2023). In addition, published genome resequencing data from 93 Chinese pangolins in non-Taiwan island (Hu et al., 2020; Wang et al., 2022b; Wei et al., 2024) and two Chinese pangolins newly sequenced in this study from Ningbo Zoo (Zhejiang, China) and Hainan Normal University (Hainan, China) were obtained. In total, 35 Chinese pangolins in Taiwan from the northern, central, southern, and eastern parts of Taiwan island, and 95 Chinese pangolins from non-Taiwan island were used for the analyses (Tables S1 and S2). The published genome data for the White-bellied pangolin (Gu et al., 2023) were used as the outgroup.

Newly generated genomic resequencing data

For samples of Chinese pangolins in Taiwan, DNA was extracted using a QIAGEN DNA purification and recovery kit, and genome resequencing was conducted by Yourgene Health in Taiwan, China. For samples of Chinese pangolins in non-Taiwan island, DNA was extracted using a Magen Hipure DNA micro-kit (Mega, China) and genome resequencing was conducted by Berry Genomics in Beijing, China. All samples were used to construct the 500 bp Illumina sequencing libraries and sequenced on the Illumina NovaSeq^{MT} platform with paired end reads of 150 bp (NCBI BioProject: PRJNA1144830). For all raw sequencing data, reads containing more than 10% ambiguous nucleotides and more than 20% low-quality nucleotides ($Q \leqslant 5$) were discarded.

SNP calling

We used BWA-MEM v.0.7.12 (Li and Durbin, 2009) to align the high-quality genome resequencing data from all samples to the chromosome-level reference genome of Chinese pangolin in Taiwan (Rhie et al., 2021). We sorted the Bam files generated by the alignment using SAMtools v.1.3 (Li et al., 2009) software in ascending order. We then used the "indelRealigner" module of GATK v.4.1.2.0 (McKenna et al., 2010) to realign the InDels in the surrounding regions, and then marked and filtered redundant sequences generated during library preparation and sequencing using the Picard software v.2.10.3 (https://broadinstitute.github.io/picard). We used the "HaplotypeCaller" module of GATK to generate gVCF files for each sample, and then combined all sample gVCF files using the "CombineGVCFs" module to obtain a population-level gVCF file. Finally, we performed variant detection using the "GenotypeGVCFs" module to obtain the original VCF file at the population level.

We filtered the original VCF file with the following parameters: "QUAL<30.0 || QD<2.0 || MQ<40.0 || FS>60.0 || SOR>3.0|| MQRankSum<–12.5 || ReadPosRankSum<–8.0 || SB⩾–1.0 || DP<3 ||MQ0⩾4 & MQ0/DP⩾0.1". Based on the chromosome-level reference genome, we retained SNPs on 19 autosomes. We removed SNPs with minor allele frequencies less than 0.05 to reduce potential false-positive sites in the sequencing. We also excluded SNPs with missing site coverage greater than 20% of samples at the population level and ensured a diploid count of two alleles within the population. In addition, we removed SNPs with sequencing depth distribution below 2.5% or above 97.5% across all sites.

Kinship analysis

Because duplicate individuals may lead to biased results in the analyses, we conducted a kinship analysis based on a genome-wide association study (KING) (Manichaikul et al., 2010) on the 35 samples collected in this study. We used the "make-king" command in PLINK v.2.0 (Purcell et al., 2007) to calculate the KING-robust coefficients between individuals, which reflects the proportion of identical SNPs between individuals. Individuals with KING-robust coefficients greater than 0.354 are considered to be identical individuals (Manichaikul et al., 2010). No identical individuals were found.

Population structure and admixture analysis

The autosomal chromosome SNPs were thinned using VCFtools v.0.1.13 (Danecek et al., 2011) based on randomly extracting a site from every 10 kb length window size to avoid the influence of linkage disequilibrium (LD) between loci, resulting in datasets of ~0.22 and ~0.01 Mb SNPs for phylogenetic analyses of Chinese

pangolin and Chinese pangolin in Taiwan, respectively. We used RAxML v.8.2.12 (Stamatakis, 2014) to build ML trees based on a GTRGAMMA model with 1,000 bootstraps. The input files used Python script vcf2phylip v.2.8 (Ortiz, 2019) to convert VCF files to PLYLIP files.

The datasets of autosomal SNPs without an outgroup were used to conduct admixture and principal component analysis (PCA) using Admixture v.1.2.3 (Alexander et al., 2009) and the smartPCA program from the Eigensoft v.4.2 package (Patterson et al., 2006), respectively. The number of ancestral clusters (K) from one to ten and the optimal K value were determined using cross-validation (Alexander et al., 2009). The PCA plots were created based on the two principal components PC1 and PC2, with the largest contributions, and the Tracy-Widom test was conducted.

Population differentiation index and migration analysis

We used a sliding-window method (50 kb window size with 25 kb window steps) to calculate the genome-wide Weir and Cockerham weighted F_{ST} value (Weir and Cockerham, 1984) to generate the differentiation index between different geographic populations of Chinese pangolin in Taiwan with VCFtools v.0.1.13 (Danecek et al., 2011). Weighted F_{ST} value ranges from 0 to 0.05, indicating that genetic differentiation between populations is too small to be considered; ranges from 0.05 to 0.15 indicate that there is a moderate degree of genetic differentiation between the populations; ranges from 0.15 to 0.25 indicate that genetic differentiation between populations is relatively large; values above 0.25 indicate that there is significant genetic differentiation between the populations (Wright, 1984). In addition, PLINK v.2.0 software (Purcell et al., 2007) was used to calculate the pairwise identity by state (IBS), which represents the consistent DNA segments within two individuals. IBS values range from 0 to 1. The lower the IBS value, the closer the relationship, and D_{IBS} (1–IBS) represents the genetic distance.

We performed a migration discontinuity test using Estimated Effective migration Surfaces (EEMS) v.0.0.0.9000 (Petkova et al., 2016) for the distribution range of Chinese pangolin in Taiwan. Based on the geographic distance and genetic distance matrix, the method identifies geographic regions where genetic similarity decays faster than expected to identify areas that have poor connectivity. We converted the SNP data for 28 out of 35 individuals with recorded geographic information into an average inverse genetic difference matrix using the bed2diffs program in EEMS. We used ArcGIS v.10.6 (https://desktop.arcgis.com/) to obtain the external coordinate file for Taiwan island. The burn-in was 2,000,000, the MCMC length was 6,000,000 iterations, and the number of grids was 500. We used the R package rEESplots v.0.0.1 (Petkova et al., 2016) for visualization.

Genetic diversity, inbreeding level, and genetic load

We assessed the genetic diversity of Chinese pangolin in Taiwan by calculating the heterozygosity (He) of all individuals. The heterozygosity for each individual was calculated based on autosomal SNPs as the ratio of the number of heterozygous sites to the number of all callable sites (Gu et al., 2023).

We evaluated the inbreeding level of Chinese pangolin in Taiwan by calculating the inbreeding coefficient (F_{ROH}) of individuals. We used PLINK v.2.0 (Purcell et al., 2007) to identify runs of homozygosity (ROHs) longer than 1 kb for each individual. The window size was set to 20 SNPs, one SNP site in the window was allowed to be a hybrid, and the number of missing sites in the window could not exceed 20%. F_{ROH} was calculated by dividing the total length of the ROHs by the total length of the autosomes covered by the SNPs (McQuillan et al., 2008). Using the physical distance of ROHs as an approximation of the genetic distance (van der Valk et al., 2019), ROHs longer than 1 Mb (g=100/2×ROH_{length}, g is the number of generations and ROH_{length} is the length of ROHs) indicated that inbreeding occurred within the last 50 years (Kardos et al., 2018).

Deleterious mutations mainly include deleterious missense mutations, loss of function (LOF) mutations, and synonymous mutations. These mutations are expected to reduce the ability to survive by disrupting gene function and are therefore considered assessment indicators of genetic load (Mattila et al., 2012). We used SnpEff v.4.3t (Cingolani et al., 2012) to classify the derived allele mutations in coding regions of each individual into LOF, missense, and synonymous mutations. We established the database based on annotation and reference genome sequences of Chinese pangolin in Taiwan (Rhie et al., 2021). The genotypes of dominant alleles in all individuals (i.e., alleles in which more than 50% of individuals are homozygous) were defined as ancestral genotypes (Feng et al., 2019). We judged whether a missense mutation was harmful based on the Grantham Score (GS) (Grantham, 1974). GS measures the physical/chemical consequences of amino acid changes. A missense mutation with GS⩾150 was considered as a deleterious missense mutation (Li et al., 1984). We estimated genetic load for each individual by calculating the ratio of the number of homozygous sites to both the homozygous and heterozygous sites for each deleterious mutation (Robinson et al., 2016).

Demographic history analyses

To infer the demographic history of Chinese pangolin in Taiwan, we used fastsimcoal2 v.2.7 (Excoffier et al., 2013) based on the joint site frequency spectrum (SFS) to evaluate the optimal population history model. We assumed that the alleles of the White-bellied pangolin outgroup were ancestral alleles and removed the heterozygote locus from the outgroup (Hu et al., 2020). We selected SNPs from a non-coding region and sites without LD affected. The final dataset of Chinese pangolin in Taiwan consists of 144,326 SNPs. EasySFS (Coffman et al., 2016) was used to obtain unfolded joint SFS from different populations. We set the mutation rate per generation to 1.47×10^{-8} (Choo et al., 2016) and the generation time to one year (Zhang et al., 2016). To identify the most suitable model, we set demographic history models with varying levels of complexity based on the number and period of different demographic historical events (Figure S6). We used 500,000 coalescent simulations and 50 optimization (ECM) cycles to run each model. To avoid local maxima, we ran 100 repetitions independently and calculated the 95% confidence intervals. We compared the fit of different models on the basis of Akaike information criterion (AIC) values (Akaike, 1974) and considered the model with the smallest AIC value to be optimal (Tables S6 and S7).

We also used GONE (Santiago et al., 2020) software, which

estimates the recent effective population size (*Ne*) based on LD, to estimate the recent *Ne* of each population of Chinese pangolin in Taiwan. GONE has been shown not to be affected by natural selection (Novo et al., 2022), and *Ne* can be estimated for small sample size populations (Santiago et al., 2020). Pairs of sites within 2 cM (parameter hc was set to 0.02) were used to reduce bias arising from recent population substructure (Santiago et al., 2020). The generation time was set to one year (Zhang et al., 2016), and other parameters used the default values. We randomly sampled 50,000 SNPs from each chromosome of each population to estimate LD, performing 40 bootstrapping iterations and calculating geometric mean values each time. The analysis was repeated 100 times for each population, and 95% confidence intervals were calculated. Finally, *Ne* values from the most recent 100 generations were estimated.

Outgroup *f3* statistic, haplotype sharing analysis, private variants, and LD decay rate

The higher the outgroup *f3* value, the closer the genetic relatedness. To infer the origin population of Chinese pangolin in Taiwan, we used AdmixTools v.7.0.2 (Patterson et al., 2012) to calculate the value of outgroup *f3* between A and B (outgroup; A, B), where the outgroup is White-bellied pangolin, A is the ancestral population, and B is each individual of 35 Chinese pangolins in Taiwan.

Furthermore, we evaluated the number of haplotypes shared between different populations of Chinese pangolin in Taiwan and the ancestor population using methods described by vonHoldt et al. (2010). Haplotype typing of SNP sites was conducted using SHAPEIT software v.5.1.0 (Delaneau et al., 2012). We selected the same number of samples for the ancestor population and each population to remove the influence of sample size. Following the recommendations associated with the software, we partitioned the genome into 20 kb non-overlapping windows and ensured that the number of SNPs in each window was equal to five (for windows with more than five SNPs, a random subset of five SNPs was chosen; windows with fewer than five SNPs were excluded). The number of shared haplotypes was denoted by the count of haplotypes present in the ancestral and each population, respectively.

We counted private variants in each population of Chinese pangolin in Taiwan using the same number of samples. Between the A and B populations, if a site was only polymorphic in the A but not in the B population, we defined it as a private variant in the A population, and *vice versa*. We also performed LD analysis for each population of Chinese pangolin in Taiwan using PopLDdecay v.3.40 (Zhang et al., 2019). We plotted the decay curve of the *r*-squared statistic (r^2), which is the correlation coefficient between two focal loci of interest.

Ecological niche modeling

We obtained 2034 distribution records for Chinese pangolin in Taiwan, including 28 records collected in this study and 2,008 records from the Taiwan Biodiversity Network (https://www.tbn.org.tw/) between 1910 and 2022. To ensure the accuracy of the results and avoid overfitting, we removed any records with unclear locations or obvious positioning errors (such as locations in the ocean), and kept only one record within every 1 km^2 (Boria et al., 2014; Lin, 2011) using the R package ENMwizard (https://github.com/HemingNM/ENMwizard/). We finally retained 390 distribution records.

To model the possible influence of historic, current, and future climatic changes on the distribution of Chinese pangolin in Taiwan, we downloaded 19 bioclimatic layers from historic periods (the LGM, approximately 22.00 kya and the MH, 7.7–6.0 kya), the current period (1970–2000), and the future period (2081–2100) with a resolution of 2.5 min (~10 km) from the WorldClim database (http://www.worldclim.org/) (Hijmans et al., 2005). We chose the farthest future climate data compared with current situation (2081 to 2100) from Worldclim to simulate future climate changes as much as possible. To avoid multicollinearity, we selected bioclimatic layers with correlations less than 0.8 ($|r|<0.8$) based on Pearson's rank correlation analyses, and the eigenvalues of PCA with a contribution of more than 10%. The results showed that three bioclimatic layers, BIO3 (Isothermality), BIO11 (Mean Temperature of Coldest Quarter), and BIO12 (Annual Precipitation), had lower correlations and could explain more than 90% of the data selected for ecological niche modeling (Table S8 and Figure S7).

We conducted ecological niche modeling in Maxent v.3.3.3e (Phillips et al., 2006). We randomly selected 80% of the distribution points to generate the training set and used the remaining 20% of the distribution points to test the effectiveness of the model. To optimize the options and settings of Maxent model and improve the accuracy of the prediction model for historical and future distributions, we investigated suitable combinations of Feature Classes (FC), which influence the shape of the response curves and Regularization Multipliers (RM), which impose penalties for the inclusion of additional parameters in the model. This evaluation was based on model performance metrics, specifically the delta value in the Akaike minimum information criterion (delta.AICc) (Zhu and Qiao, 2016). We identified the best model using the R package ENMeval v.2.0.4 (https://cran.r-project.org/web/packages/ENMeval/index.html/) (Muscarella et al., 2014) with the "ENMevaluate" function. The FC used was "L", "H", "LQ", "LQH", "LQHP", "LQHTP" (where L=linear, Q=quadratic, H=hinge, P=product and T=threshold), and the RM values (0.5, 1, 1.5, 2, 2.5, 3, 3.5, 4). The result showed that the combination of H (FC) and 1 (RM) was the best (Figure S8). We then used the optimal combination of FC and RM with the rest of the default parameters for ecological niche modeling (Phillips and Dudík, 2008). Each model was independently run 20 times. We used the maximum training sensitivity plus specificity threshold (MaxSS) to translate continuous ecological niche modeling into predictions of species presence (1) and absence (0) (Liu et al., 2013). We used ArcGIS 10.6 to visualize the output models.

We used three general circulation models (GCMs) (MPI-ESM-P, CCSM4, and MIROC-ESM) for both the MH and LGM climate scenarios. The highest value of area under the receiver operating characteristic curve (AUC, 0.7–0.8 indicates acceptable performance, 0.8–0.9 indicates excellent performance, and >0.9 indicates outstanding performance (Phillips et al., 2006)) was used to evaluate the best model (Table S9). When estimating the future distribution, we also included land cover factors that may directly or indirectly affect species distribution by affecting food availability (Wisz et al., 2013). Land cover data were obtained from the Land Use Harmonization2 project (http://luh.umd.edu/) at a resolution of 2.5 min to match the bioclimatic layers. Two types of land cover, grassland, and

forest, were selected for ecological niche modeling as well as bioclimatic layers (Table S10 and Figure S9). We selected model INM-CM5-0 of the CMIP6 climate model with two different shared socioeconomic pathway scenarios (SSP1-2.6 and SSP5-8.5) (Riahi et al., 2017) for future distribution projections of each population (Table S8), respectively. The INM-CM5-0 model performs well in predicting precipitation (Wang et al., 2022a), which was the bioclimatic layer (BIO12, 49.74%) that contributed most in the PCA. SSP5-8.5 represents the worst-case greenhouse effect with an increased average annual temperature of 2.4–4.8°C above the current level in 2081–2100. SSP1-2.6 is a more optimistic scenario, with average annual temperature only increasing by 0.5–1.5°C compared with the current level in 2081–2100 (Intergovernmental Panel on Climate Change (IPCC), 2023).

Identification of SNPs associated with climate adaptation

To control the high false positive rate in the identification of the climate-associated SNPs (Rellstab et al., 2015), we used both LFMM (Frichot et al., 2013) and RDA (Forester et al., 2016) approaches to identify SNPs that were significantly associated with BIO3, BIO11, and BIO12. We first used the R package lfmm v.1.1 (https://CRAN.R-project.org/package=lfmm), with the latent factor K set to the number of genetic populations and the remaining parameters set to the defaults. We retained SNPs with P values less than 0.05 for all three environmental variables. Then we carried out RDA analyses with the R package vegan v.2.6-4 (https://CRAN.R-project.org/package=vegan), with the constrained axes K also set to the number of genetic populations. We retained SNPs with P values and Q values less than 0.05. We identified the SNPs that were significant in both methods as climate-associated SNPs.

Genetic offset modeling

For the identified climate-associated SNPs, we used GF v.0.1.37 (https://r-forge.r-project.org/projects/gradientforest/) (Ellis et al., 2012) to estimate the genetic offsets for Chinese pangolin in Taiwan in response to future climate changes. We used 500 regression trees to build a function for each SNP for each climatic variable and set the correlation threshold to 0.5. To explore future climate impacts on Chinese pangolin in Taiwan, we used two shared socioeconomic pathway scenarios (SSP1-2.6 and SSP5-8.5) in the INM-CM5-0 climate model to predict genetic offsets in 2081–2100. We assessed the geographical areas in which the relationship between genotype and climate is likely to be most significantly altered in the context of future climatic conditions using local genetic offsets (Fitzpatrick and Keller, 2015). In this analysis, local genetic offsets were determined by forecasting genetic differentiation for climate-associated SNPs between present and anticipated future climates at identical locations. This calculation employed multidimensional Euclidean distance for genetic factors, under the assumption of no dispersal or gene flow.

Future evolutionary potential simulation

We used the SLiM v.3.6 software (Haller and Messer, 2019) to simulate the future evolutionary potential (e.g., deleterious mutations, inbreeding coefficient, heterozygosity, fitness) for each population under a Wright-Fisher model. We set the effective population sizes (*Ne*) of our simulations according to the best demographic model for each population (Figure 5A) and used different models to simulate the evolutionary potential under different growth rates of *Ne* (1%, 3%, 5%, and 7%) in the next century. Based on the genome characteristics of the Chinese pangolin in Taiwan, we simulated a genome containing 19 chromosomes and 20,000 genes, the length for each gene was 1,500 bp (Xie et al., 2022), and the number of genes was proportional to the length of the chromosome (Xie et al., 2022). The mutation rate was 1.47×10^{-8} per site per generation (Choo et al., 2016), the generation time was one year (Zhang et al., 2016), the genetic recombination rate was 1×10^{-3} per site per generation, and the ratio of deleterious (non-synonymous) mutations to neutral (synonymous) mutations was set to 2.31:1 (Huber et al., 2017). The dominance coefficient (h) and the selection coefficient (s) were set to be inversely related, given that highly deleterious mutations tend to be highly recessive. Specifically, we assumed h=0.01 (s<–0.01) for strong deleterious mutations; h=0.1 (–0.01⩽s<–0.001) for medium deleterious mutations; h=0.4 (s>–0.001) for weak deleterious mutations (Dussex et al., 2021). For all simulated scenarios, we conducted 25 runs, outputting results every 10 generations. We calculated the average and 95% confidence interval for the results of all runs. The mean heterozygosity, F_{ROH} (calculated using ROHs>100 kb to monitor recent inbreeding), genetic load, and population fitness were also calculated.

Data and code availability

The resequencing short-read Fastq files generated in this study have been deposited to the NCBI (https://www.ncbi.nlm.nih.gov/) archive under project PRJNA1144830. The reference genome of Chinese pangolin in Taiwan (PRJNA924339) was downloaded from https://www.ncbi.nlm.nih.gov/bioproject/PRJNA924339 (Rhie et al., 2021). Previously published data used for this work (PRJNA20331, PRJNA512907, PRJNA529540, CNP0001723 and PRJNA962256) were downloaded from https://www.ncbi.nlm.nih.gov/bioproject/PRJNA20331 (Choo et al., 2016), https://www.ncbi.nlm.nih.gov/bioproject/PRJNA512907 (Houck et al., 2023), https://www.ncbi.nlm.nih.gov/bioproject/PRJNA529540 (Hu et al., 2020), https://db.cngb.org/search/project/CNP0001723 (Wang et al., 2022b; Wei et al., 2024) and https://www.ncbi.nlm.nih.gov/bioproject/PRJNA962256 (Gu et al., 2023). Tissue samples in this study were obtained from individuals involved in road accidents and stored in absolute ethanol or as material stored at –20°C. Code for data processing and analysis, and simulations used in this study have been deposited in GitHub (https://github.com/Zhaitianya428/Chinese_pangolin_in_Taiwan).

Compliance and ethics

The authors declare that they have no conflict of interest. All necessary research permits and ethical approvals have been obtained from Yunnan University for this study (No. YNU20240774).

Acknowledgement

This work was supported by the National Natural Science Foundation of China (32470527, 32160130), Xingdian Talent Fund Project of Yunnan Province, Basic Research of Yunnan Province (202301AT070185), Joint Funding of the Yunnan Provincial Science and Technology Department and Yunnan University (202401BF070001-018), Wildlife Protection Administration of Hainan Province, Scientific Research and Innovation Project of Postgraduate Students in the Academic Degree of Yunnan University (KC-23234049), and Central Government Guidance Fund for the Development of Local Science and Technology (202407AB110004).

Supporting information

The supporting information is available online at https://doi.org/10.1007/s11427-024-2904-6. The supporting materials are published as submitted, without typesetting or editing. The responsibility for scientific accuracy and content remains entirely with the authors.

References

Adams, N.E., and Edmands, S. (2023). Genomic recovery lags behind demographic recovery in bottlenecked populations of the Channel Island fox, *Urocyon littoralis*. Mol Ecol 32, 4151–4164.

Akaike, H. (1974). A new look at the statistical model identification. IEEE Trans Automat Contr 19, 716–723.

Alexander, D.H., Novembre, J., and Lange, K. (2009). Fast model-based estimation of ancestry in unrelated individuals. Genome Res 19, 1655–1664.

Allen, G.M. (1938). The mammals of China and Mongolia (New York: American Museum of Natural History).

Antevs, E. (1953). Tree-rings and seasons in past geologic eras. Tree-Ring Bull 20, 17–19.

Berends, C.J., de Boer, B., and van de Wal, R.S.W. (2021). Reconstructing the evolution of ice sheets, sea level, and atmospheric CO_2 during the past 3.6 million years. Clim Past 17, 361–377.

Bintanja, R., van de Wal, R.S.W., and Oerlemans, J. (2005). Modelled atmospheric temperatures and global sea levels over the past million years. Nature 437, 125–128.

Boria, R.A., Olson, L.E., Goodman, S.M., and Anderson, R.P. (2014). Spatial filtering to reduce sampling bias can improve the performance of ecological niche models. Ecol Model 275, 73–77.

Buckland, S., Cole, N.C., Groombridge, J.J., Küpper, C., Burke, T., Dawson, D.A., Gallagher, L.E., Harris, S., and Pinto, J. (2014). High risks of losing genetic diversity in an endemic Mauritian Gecko: implications for conservation. PLoS One 9, e93387.

Butchart, S.H.M., Walpole, M., Collen, B., van Strien, A., Scharlemann, J.P.W., Almond, R.E.A., Baillie, J.E.M., Bomhard, B., Brown, C., Bruno, J., et al. (2010). Global biodiversity: indicators of recent declines. Science 328, 1164–1168.

Ceballos, G., Ehrlich, P.R., Barnosky, A.D., García, A., Pringle, R.M., and Palmer, T.M. (2015). Accelerated modern human-induced species losses: entering the sixth mass extinction. Sci Adv 1, e1400253.

Ceballos, G., Ehrlich, P.R., and Dirzo, R. (2017). Biological annihilation via the ongoing sixth mass extinction signaled by vertebrate population losses and declines. Proc Natl Acad Sci USA 114, E6089.

Challender, D.W.S., Harrop, S.R., and MacMillan, D.C. (2015). Understanding markets to conserve trade-threatened species in CITES. Biol Conservation 187, 249–259.

Challender, D.W.S., Nash, H.C., and Waterman, C. (2020). Pangolins: Science, Society and Conservation (London, San Diego, CA: Academic Press).

Challender, D.W.S., Wu, S., Kaspal, P., Khatiwada, A., Ghose, A., Sun, C.M., Mohapatra, R.K., and Suwal, T.L. (2019). IUCN red list of threatened species: *Manis pentadactyla*. The IUCN Red List of Threatened Species. Available from URL: https://www.iucnredlist.org.

Chang, A.Y., Chen, W.J., He, R.Y., Lin, D.L., Lin, Y.L., Lin, T.E., Chou, S.P., Lin, C.F., Lin, R.S., ChangChien, L.W., et al. (2022). Range map datasets for terrestrial vertebrates across Taiwan. Data Brief 42, 108060.

Chao, J.T. (1989). Studies on the Conservation of the Pangolin in Taiwan (*Manis pentadactyla pentadactyla*) (Taiwan, China: Division of forest biology, Taiwan Forestry Research Institute).

Chen, J.H., Huang, C.L., Lai, Y.L., Chang, C.T., Liao, P.C., Hwang, S.Y., and Sun, C.W. (2017a). Postglacial range expansion and the role of ecological factors in driving adaptive evolution of *Musa basjoo* var. formosana. Sci Rep 7, 5341.

Chen, P.C., Shih, C.H., Chu, T.J., Lee, Y.C., Tzeng, T.D., and Chiang, T.Y. (2017b). Phylogeography and genetic structure of the oriental river prawn *Macrobrachium nipponense* (Crustacea: Decapoda: Palaemonidae) in East Asia. PLoS One 12, e0173490.

Cheng, Y., Hwang, S., and Lin, T. (2005). Potential refugia in Taiwan revealed by the phylogeographical study of *Castanopsis carlesii* Hayata (Fagaceae). Mol Ecol 14, 2075–2085.

Choo, S.W., Rayko, M., Tan, T.K., Hari, R., Komissarov, A., Wee, W.Y., Yurchenko, A. A., Kliver, S., Tamazian, G., Antunes, A., et al. (2016). Pangolin genomes and the evolution of mammalian scales and immunity. Genome Res 26, 1312–1322.

Cingolani, P., Platts, A., Wang, L.L., Coon, M., Nguyen, T., Wang, L., Land, S.J., Lu, X., and Ruden, D.M. (2012). A program for annotating and predicting the effects of single nucleotide polymorphisms, SnpEff: SNPs in the genome of Drosophila melanogaster strain w1118; iso-2; iso-3. Fly 6, 80–92.

Coffman, A.J., Hsieh, P.H., Gravel, S., and Gutenkunst, R.N. (2016). Computationally efficient composite likelihood statistics for demographic inference. Mol Biol Evol 33, 591–593.

Cooke, S.B., Dávalos, L.M., Mychajliw, A.M., Turvey, S.T., and Upham, N.S. (2017). Anthropogenic extinction dominates holocene declines of West Indian mammals. Annu Rev Ecol Evol Syst 48, 301–327.

Crooks, K.R., Burdett, C.L., Theobald, D.M., King, S.R.B., Di Marco, M., Rondinini, C., and Boitani, L. (2017). Quantification of habitat fragmentation reveals extinction risk in terrestrial mammals. Proc Natl Acad Sci USA 114, 7635–7640.

Cruz Berrocal, M., Serrano Herrero, E., Gener Moret, M., Uriarte González, A., Torra Pérez, M., Consuegra Rodríguez, S., Chevalier, A., Valentin, F., and Tsang, C. (2018). A comprised archaeological history of Taiwan through the long-term record of Heping Dao, Keelung. Int J Histor Archaeol 22, 905–940.

Danecek, P., Auton, A., Abecasis, G., Albers, C.A., Banks, E., DePristo, M.A., Handsaker, R.E., Lunter, G., Marth, G.T., Sherry, S.T., et al. (2011). The variant call format and VCFtools. Bioinformatics 27, 2156–2158.

Delaneau, O., Marchini, J., and Zagury, J.F. (2012). A linear complexity phasing method for thousands of genomes. Nat Methods 9, 179–181.

Dussex, N., van der Valk, T., Morales, H.E., Wheat, C.W., Díez-del-Molino, D., von Seth, J., Foster, Y., Kutschera, V.E., Guschanski, K., Rhie, A., et al. (2021). Population genomics of the critically endangered kākāpō. Cell Genomics 1, 100002.

Ellerman, J.R., and Morrison-Scott, T.C.S. (1951). Checklist of Palaearctic and Indian Mammals 1758 to 1946 (London: Natural History Museum (London) Publications).

Ellis, N., Smith, S.J., and Pitcher, C.R. (2012). Gradient forests: calculating importance gradients on physical predictors. Ecology 93, 156–168.

Excoffier, L., Dupanloup, I., Huerta-Sánchez, E., Sousa, V.C., Foll, M., and Akey, J.M. (2013). Robust demographic inference from genomic and SNP data. PLoS Genet 9, e1003905.

Feng, S., Fang, Q., Barnett, R., Li, C., Han, S., Kuhlwilm, M., Zhou, L., Pan, H., Deng, Y., Chen, G., et al. (2019). The genomic footprints of the fall and recovery of the crested ibis. Curr Biol 29, 340–349.e7.

Fitzpatrick, M.C., and Keller, S.R. (2015). Ecological genomics meets community-level modelling of biodiversity: mapping the genomic landscape of current and future environmental adaptation. Ecol Lett 18, 1–16.

Forester, B.R., Jones, M.R., Joost, S., Landguth, E.L., and Lasky, J.R. (2016). Detecting spatial genetic signatures of local adaptation in heterogeneous landscapes. Mol Ecol 25, 104–120.

Frankham, R., Ballou, J.D., and Briscoe, D.A. (2002). Introduction to Conservation Genetics (Cambridge: Cambridge University Press).

Frichot, E., Schoville, S.D., Bouchard, G., and François, O. (2013). Testing for associations between loci and environmental gradients using latent factor mixed models. Mol Biol Evol 30, 1687–1699.

Funk, W.C., McKay, J.K., Hohenlohe, P.A., and Allendorf, F.W. (2012). Harnessing genomics for delineating conservation units. Trends Ecol Evol 27, 489–496.

Grantham, R. (1974). Amino acid difference formula to help explain protein evolution. Science 185, 862–864.

Gu, T.T., Wu, H., Yang, F., Gaubert, P., Heighton, S.P., Fu, Y., Liu, K., Luo, S.J., Zhang, H.R., Hu, J.Y., et al. (2023). Genomic analysis reveals a cryptic pangolin species. Proc Natl Acad Sci USA 120, e2304096120.

Haller, B.C., and Messer, P.W. (2019). SLiM 3: forward genetic simulations beyond the wright-fisher model. Mol Biol Evol 36, 632–637.

Hedrick, P.W., Gutierrez-Espeleta, G.A., and Lee, R.N. (2001). Founder effect in an island population of bighorn sheep. Mol Ecol 10, 851–857.

Heinen, J.H., van Loon, E.E., Hansen, D.M., and Kissling, W.D. (2018). Extinction-driven changes in frugivore communities on oceanic islands. Ecography 41, 1245–1255.

Hijmans, R.J., Cameron, S.E., Parra, J.L., Jones, P.G., and Jarvis, A. (2005). Very high resolution interpolated climate surfaces for global land areas. Int J Climatol 25, 1965–1978.

Hohenlohe, P.A., Funk, W.C., and Rajora, O.P. (2021). Population genomics for wildlife conservation and management. Mol Ecol 30, 62–82.

Holdaway, R.N., and Jacomb, C. (2000). Rapid extinction of the Moas (Aves: Dinornithiformes): model, test, and implications. Science 287, 2250–2254.

Houck, M.L., Koepfli, K.P., Hains, T., Khan, R., Charter, S.J., Fronczek, J.A., Misuraca, A.C., Kliver, S., Perelman, P.L., Beklemisheva, V., et al. (2023). Chromosome-length genome assemblies and cytogenomic analyses of pangolins reveal remarkable chromosome counts and plasticity. Chromosome Res 31, 13.

Hsu, F.H., Lin, F., and Lin, Y.S. (2001). Phylogeographic structure of the wood mouse in Taiwan, *Apodemus semotus* Thomas. Zool Stud 40, 91–102.

Hu, J.Y., Hao, Z.Q., Frantz, L., Wu, S.F., Chen, W., Jiang, Y.F., Wu, H., Kuang, W.M., Li, H., Zhang, Y.P., et al. (2020). Genomic consequences of population decline in critically endangered pangolins and their demographic histories. Natl Sci Rev 7, 798–814.

Huang, J.P., and Lin, C.P. (2011). Lineage-specific late pleistocene expansion of an endemic subtropical gossamer-wing damselfly, *Euphaea formosa*, in Taiwan. BMC Evol Biol 11, 94.

Huang, S.S.F., Hwang, S., and Lin, T. (2002). Spatial pattern of chloroplast DNA variation of *Cyclobalanopsis glauca* in Taiwan and East Asia. Mol Ecol 11, 2349–2358.
Huber, C.D., Kim, B.Y., Marsden, C.D., and Lohmueller, K.E. (2017). Determining the factors driving selective effects of new nonsynonymous mutations. Proc Natl Acad Sci USA 114, 4465–4470.
Intergovernmental Panel on Climate Change (IPCC). (2023). Climate Change 2021—The Physical Science Basis: Working Group I Contribution to the Sixth Assessment Report of the Intergovernmental Panel on Climate Change (Cambridge: Cambridge University Press).
Ju, Y.M., Hsu, K.C., Yang, J.Q., Wu, J.H., Li, S., Wang, W.K., Ding, F., Li, J., and Lin, H. D. (2018). Mitochondrial diversity and phylogeography of *Acrossocheilus paradoxus* (Teleostei: Cyprinidae). Mitochondrial DNA Part A 29, 1194–1202.
Kao, J., Chao, J.T., Chin, J.S.C., Jang-Liaw, N.H., Li, J.Y.W., Lees, C., Traylor-Holzer, K., Chen, T.T.Y., and Lo, F.H.Y. (2020). Chapter 36 - Conservation planning and PHVAs in Taiwan. In Pangolins: Science, Society and Conservation. Biodiversity of World: Conservation From Genes to Landscapes, D.W.S. Challender, H.C. Nash, and C. Waterman, ed. (London, San Diego, CA: Academic Press), pp. 559–577.
Kao, J., Li, J.Y.W., Lees, C., Traylor-Holzer, K., Jang-Liaw, N.H., Chen, T.T.Y., Lo, F.H. Y., Yu, H.Y., and Sun, C.M. (2019). 2017 Population and habitat viability assessment and conservation action plan for the pangolin in Taiwan, *Manis p. pentadactyla*. Apple Valley: IUCN SSC Conservation Planning Specialist Group.
Kardos, M., Åkesson, M., Fountain, T., Flagstad, Ø., Liberg, O., Olason, P., Sand, H., Wabakken, P., Wikenros, C., and Ellegren, H. (2018). Genomic consequences of intensive inbreeding in an isolated wolf population. Nat Ecol Evol 2, 124–131.
Kaufman, D.S., and Broadman, E. (2023). Revisiting the Holocene global temperature conundrum. Nature 614, 425–435.
Kier, G., Kreft, H., Lee, T.M., Jetz, W., Ibisch, P.L., Nowicki, C., Mutke, J., and Barthlott, W. (2009). A global assessment of endemism and species richness across island and mainland regions. Proc Natl Acad Sci USA 106, 9322–9327.
Kyriazis, C.C., Beichman, A.C., Brzeski, K.E., Hoy, S.R., Peterson, R.O., Vucetich, J.A., Vucetich, L.M., Lohmueller, K.E., Wayne, R.K., and Nielsen, R. (2023). Genomic underpinnings of population persistence in Isle Royale moose. Mol Biol Evol 40, msad021.
Leclerc, C., Courchamp, F., and Bellard, C. (2020). Future climate change vulnerability of endemic island mammals. Nat Commun 11, 4943.
Li, H., and Durbin, R. (2009). Fast and accurate short read alignment with Burrows-Wheeler transform. Bioinformatics 25, 1754–1760.
Li, H., Handsaker, B., Wysoker, A., Fennell, T., Ruan, J., Homer, N., Marth, G., Abecasis, G., and Durbin, R. (2009). The sequence alignment/map format and SAMtools. Bioinformatics 25, 2078–2079.
Li, K.Y., Hsiao, C., Yen, S.C., Hung, C.Y., Lin, Y.Z., Jheng, S.W., Yu, P.J., Hwang, M.H., Weng, G.J., Chen, K.L., et al. (2023). Phylogenetic divergence associated with climate oscillations and topology illustrates the dispersal history of sambar deer (*Rusa unicolor swinhoii*) in Taiwan. Mamm Res 68, 283–294.
Li, W.H., Wu, C.I., and Luo, C.C. (1984). Nonrandomness of point mutation as reflected in nucleotide substitutions in pseudogenes and its evolutionary implications. J Mol Evol 21, 58–71.
Lin, J.S. (2011). Home range and burrow utilization in pangolin in Taiwan (*Manis pentadactyla pentadactyla*) at Luanshan, Taitung (in Chinese). Dissertation for Master's Degree. (Taiwan, China: Pingtung University of Science and Technology).
Liu, C., White, M., Newell, G., and Pearson, R. (2013). Selecting thresholds for the prediction of species occurrence with presence-only data. J Biogeogr 40, 778–789.
Liu, J.T. (2017). Genetic diversity and genetic structure of pangolin in Taiwan based on MHC gene and microsatellite markers (in Chinese). Dissertation for Master's Degree. (Taiwan, China: Taiwan University).
Mack, A.L., and Wright, D.D. (1998). The vulturine parrot, *Psittrichas fulgidus*, a threatened New Guinea endemic: notes on its biology and conservation. Bird Conserv Int 8, 185–194.
Manes, S., Costello, M.J., Beckett, H., Debnath, A., Devenish-Nelson, E., Grey, K.A., Jenkins, R., Khan, T.M., Kiessling, W., Krause, C., et al. (2021). Endemism increases species' climate change risk in areas of global biodiversity importance. Biol Conserv 257, 109070.
Manichaikul, A., Mychaleckyj, J.C., Rich, S.S., Daly, K., Sale, M., and Chen, W.M. (2010). Robust relationship inference in genome-wide association studies. Bioinformatics 26, 2867–2873.
Matthews, T.J., Triantis, K.A., and Whittaker, R.J. (2021). The Species-Area Relationship: Theory and Application (Cambridge: Cambridge University Press).
Mattila, A.L.K., Duplouy, A., Kirjokangas, M., Lehtonen, R., Rastas, P., and Hanski, I. (2012). High genetic load in an old isolated butterfly population. Proc Natl Acad Sci USA 109, E2496.
Maunder, Culham, Bordeu, Allainguillaume, and Wilkinson (1999). Genetic diversity and pedigree for *Sophora toromiro* (Leguminosae): a tree extinct in the wild. Mol Ecol 8, 725–738.
Mayr, E. (2013). Animal Species and Evolution (Cambridge: Harvard University Press).
McKenna, A., Hanna, M., Banks, E., Sivachenko, A., Cibulskis, K., Kernytsky, A., Garimella, K., Altshuler, D., Gabriel, S., Daly, M., et al. (2010). The Genome Analysis Toolkit: a MapReduce framework for analyzing next-generation DNA sequencing data. Genome Res 20, 1297–1303.
McQuillan, R., Leutenegger, A.L., Abdel-Rahman, R., Franklin, C.S., Pericic, M., Barac-Lauc, L., Smolej-Narancic, N., Janicijevic, B., Polasek, O., Tenesa, A., et al. (2008). Runs of homozygosity in European populations. Am J Hum Genet 83, 658.
Muscarella, R., Galante, P.J., Soley-Guardia, M., Boria, R.A., Kass, J.M., Uriarte, M., Anderson, R.P., and McPherson, J. (2014). ENM eval: an R package for conducting spatially independent evaluations and estimating optimal model complexity for Maxent ecological niche models. Methods Ecol Evol 5, 1198–1205.
Novo, I., Santiago, E., Caballero, A., and Payseur, B. (2022). The estimates of effective population size based on linkage disequilibrium are virtually unaffected by natural selection. PLoS Genet 18, e1009764.
Orkin, J.D., Kuderna, L.F.K., Hermosilla-Albala, N., Fontsere, C., Aylward, M.L., Janiak, M.C., Andriaholinirina, N., Balaresque, P., Blair, M.E., Fausser, J.L., et al. (2025). Ecological and anthropogenic effects on the genomic diversity of lemurs in Madagascar. Nat Ecol Evol 9, 42–56.
Ortiz, E.M. (2019). vcf2phylip v2.0: Convert a VCF matrix into several matrix formats for phylogenetic analysis. Zenodo. Available from URL: https://zenodo.org/records/2540861.
Oshida, T., Lee, J.K., Lin, L.K., and Chen, Y.J. (2006). Phylogeography of pallas's squirrel in Taiwan: geographical isolation in an arboreal small mammal. J Mammal 87, 247–254.
Patterson, N., Moorjani, P., Luo, Y., Mallick, S., Rohland, N., Zhan, Y., Genschoreck, T., Webster, T., and Reich, D. (2012). Ancient admixture in human history. Genetics 192, 1065–1093.
Patterson, N., Price, A.L., and Reich, D. (2006). Population structure and eigenanalysis. PLoS Genet 2, e190.
Petkova, D., Novembre, J., and Stephens, M. (2016). Visualizing spatial population structure with estimated effective migration surfaces. Nat Genet 48, 94–100.
Phillips, S.J., Anderson, R.P., and Schapire, R.E. (2006). Maximum entropy modeling of species geographic distributions. Ecol Model 190, 231–259.
Phillips, S.J., and Dudík, M. (2008). Modeling of species distributions with Maxent: new extensions and a comprehensive evaluation. Ecography 31, 161–175.
Pimm, S.L., Jenkins, C.N., Abell, R., Brooks, T.M., Gittleman, J.L., Joppa, L.N., Raven, P.H., Roberts, C.M., and Sexton, J.O. (2014). The biodiversity of species and their rates of extinction, distribution, and protection. Science 344, 1246752.
Purcell, S., Neale, B., Todd-Brown, K., Thomas, L., Ferreira, M.A.R., Bender, D., Maller, J., Sklar, P., de Bakker, P.I.W., Daly, M.J., et al. (2007). PLINK: a tool set for whole-genome association and population-based linkage analyses. Am J Hum Genet 81, 559–575.
Qiu, J., Jin, J., Wang, X., Wei, C., Zuo, X., and Wei, J. (2023). OSL chronological evidence reveals one of the earliest island-type Neolithic sites in the coastal area of South China. Holocene 33, 27–37.
Rellstab, C., Gugerli, F., Eckert, A.J., Hancock, A.M., and Holderegger, R. (2015). A practical guide to environmental association analysis in landscape genomics. Mol Ecol 24, 4348–4370.
Rhie, A., McCarthy, S.A., Fedrigo, O., Damas, J., Formenti, G., Koren, S., Uliano-Silva, M., Chow, W., Fungtammasan, A., Kim, J., et al. (2021). Towards complete and error-free genome assemblies of all vertebrate species. Nature 592, 737–746.
Riahi, K., van Vuuren, D.P., Kriegler, E., Edmonds, J., O'Neill, B.C., Fujimori, S., Bauer, N., Calvin, K., Dellink, R., Fricko, O., et al. (2017). The Shared Socioeconomic Pathways and their energy, land use, and greenhouse gas emissions implications: an overview. Glob Environ Change 42, 153–168.
Robinson, J.A., Ortega-Del Vecchyo, D., Fan, Z., Kim, B.Y., vonHoldt, B.M., Marsden, C.D., Lohmueller, K.E., and Wayne, R.K. (2016). Genomic flatlining in the endangered island fox. Curr Biol 26, 1183–1189.
Robinson, J.A., Brown, C., Kim, B.Y., Lohmueller, K.E., and Wayne, R.K. (2018). Purging of strongly deleterious mutations explains long-term persistence and absence of inbreeding depression in island foxes. Curr Biol 28, 3487–3494.e4.
Robinson, J.A., Räikkönen, J., Vucetich, L.M., Vucetich, J.A., Peterson, R.O., Lohmueller, K.E., and Wayne, R.K. (2019). Genomic signatures of extensive inbreeding in Isle Royale wolves, a population on the threshold of extinction. Sci Adv 5, eaau0757.
Santiago, E., Novo, I., Pardiñas, A.F., Saura, M., Wang, J., Caballero, A., and Kim, Y. (2020). Recent demographic history inferred by high-resolution analysis of linkage disequilibrium. Mol Biol Evol 37, 3642–3653.
Schrader, J., Weigelt, P., Cai, L., Westoby, M., Fernández-Palacios, J.M., Cabezas, F.J., Plunkett, G.M., Ranker, T.A., Triantis, K.A., Trigas, P., et al. (2024). Islands are key for protecting the world's plant endemism. Nature 634, 868–874.
Stamatakis, A. (2014). RAxML version 8: a tool for phylogenetic analysis and post-

analysis of large phylogenies. Bioinformatics 30, 1312–1313.
Sun, C.M., Chang, S.P., Lin, J.S., Tseng, Y.W., Pei, K.J.C., and Hung, K.H. (2020). The genetic structure and mating system of a recovered Chinese pangolin population (*Manis pentadactyla* Linnaeus, 1758) as inferred by microsatellite markers. Glob Ecol Conserv 23, e01195.
Sun, N., Huang, C.C., Tseng, Y.W., Laxmi Suwal, T., Chi, M.J., Jang-Liaw, N.H., and Hung, K.H. (2021). Complete mitochondrial genome of *Manis pentadactyla pentadactyla* (Mammalia: Pholidota), an endemic subspecies of Chinese pangolin: mitogenome characterisation and phylogenetic implications. BDJ 9, e77961.
Tershy, B.R., Shen, K.W., Newton, K.M., Holmes, N.D., and Croll, D.A. (2015). The importance of islands for the protection of biological and linguistic diversity. Bioscience 65, 592–597.
Toda, M., Nishida, M., Matsui, M., Lue, K.Y., and Ota, H. (1998). Genetic variation in the Indian rice frog, *Rana limnocharis* (Amphibia: Anura), in Taiwan, as revealed by allozyme data. Herpetologica 54, 73–82.
van Daalen, K.R., Tonne, C., Semenza, J.C., Rocklöv, J., Markandya, A., Dasandi, N., Jankin, S., Achebak, H., Ballester, J., Bechara, H., et al. (2024). The 2024 Europe report of the *Lancet* Countdown on health and climate change: unprecedented warming demands unprecedented action. Lancet Public Health 9, e495–e522.
van der Valk, T., Díez-del-Molino, D., Marques-Bonet, T., Guschanski, K., and Dalén, L. (2019). Historical genomes reveal the genomic consequences of recent population decline in eastern gorillas. Curr Biol 29, 165–170.e6.
Vidal, F., van der Marel, E.R., Kerr, R.W.F., McElroy, C., Schroeder, N., Mitchell, C., Rosetto, G., Chen, T.T.D., Bailey, R.M., Hepburn, C., et al. (2024). Designing a circular carbon and plastics economy for a sustainable future. Nature 626, 45–57.
vonHoldt, B.M., Pollinger, J.P., Lohmueller, K.E., Han, E., Parker, H.G., Quignon, P., Degenhardt, J.D., Boyko, A.R., Earl, D.A., Auton, A., et al. (2010). Genome-wide SNP and haplotype analyses reveal a rich history underlying dog domestication. Nature 464, 898–902.
Walker, M.J.C., Berkelhammer, M., Björck, S., Cwynar, L.C., Fisher, D.A., Long, A.J., Lowe, J.J., Newnham, R.M., Rasmussen, S.O., and Weiss, H. (2012). Formal subdivision of the Holocene Series/Epoch: a discussion paper by a working group of INTIMATE (Integration of ice-core, marine and terrestrial records) and the subcommission on quaternary stratigraphy (International Commission on Stratigraphy). J Quat Sci 27, 649–659.
Waller, N.L., Gynther, I.C., Freeman, A.B., Lavery, T.H., and Leung, L.K.P. (2017). The Bramble Cay melomys *Melomys rubicola* (Rodentia: Muridae): a first mammalian extinction caused by human-induced climate change? Wildl Res 44, 9.
Wang, L., Li, Y., Li, M., Li, L., Liu, F., Liu, D.L., and Pulatov, B. (2022a). Projection of precipitation extremes in China's mainland based on the statistical downscaled data from 27 GCMs in CMIP6. Atmos Res 280, 106462.
Wang, P.J. (2007). Application of wildlife rescue system in conservation of the pangolin in Taiwan (*Manis pentadactyla pentadactyla*) (in Chinese). Dissertation for Master's Degree. (Taiwan, China: Taiwan University).
Wang, Q., Lan, T., Li, H., Sahu, S.K., Shi, M., Zhu, Y., Han, L., Yang, S., Li, Q., Zhang, L., et al. (2022b). Whole-genome resequencing of Chinese pangolins reveals a population structure and provides insights into their conservation. Commun Biol 5, 821.
Wei, S., Fan, H., Zhou, W., Huang, G., Hua, Y., Wu, S., Wei, X., Chen, Y., Tan, X., and Wei, F. (2024). Conservation genomics of the critically endangered Chinese pangolin. Sci China Life Sci 67, 2051–2061.
Weir, B.S., and Cockerham, C.C. (1984). Estimating F-statistics for the analysis of population structure. Evolution 38, 1358–1370.
Weng, G.J., Liu, J.N., and DuanMu, M.N. (2023). Optimization of the long-term wildlife monitoring system and data integration (in Chinese). Taiwan Pingtung University of Science and Technology, Taiwan Chiayi University and Academia Sinica. Report No.: 112-7.2.6-e1.
Whittaker, R.J., Fernández-Palacios, J.M., Matthews, T.J., Borregaard, M.K., and Triantis, K.A. (2017). Island biogeography: taking the long view of nature's laboratories. Science 357, eaam8326.
Willcox, D., Nash, H.C., Trageser, S., Kim, H.J., Hywood, L., Connelly, E., Ichu Ichu, G., Kambale Nyumu, J., Mousset Moumbolou, C.L., Ingram, D.J., et al. (2019). Evaluating methods for detecting and monitoring pangolin (Pholidata: Manidae) populations. Glob Ecol Conserv 17, e00539.
Wilson, D.E., and Reeder, D.M. (2005). Mammal Species of the World: A Taxonomic and Geographic Reference. 3rd ed. (Baltimore: Johns Hopkins University Press).
Wisz, M.S., Pottier, J., Kissling, W.D., Pellissier, L., Lenoir, J., Damgaard, C.F., Dormann, C.F., Forchhammer, M.C., Grytnes, J., Guisan, A., et al. (2013). The role of biotic interactions in shaping distributions and realised assemblages of species: implications for species distribution modelling. Biol Rev 88, 15–30.
Wright, S. (1984). Evolution and the Genetics of Populations, Volume 4: Variability Within and Among Natural Populations (Chicago: University of Chicago Press).
Wu, S.H., Chen, M., Chin, S., Lee, D.J., Wen, P.Y., Chen, L.W., Wang, B.T., and Yu H. T. (2007). Cytogenetic analysis of the pangolin in Taiwan, *Manis pentadactyla pentadactyla* (Mammalia: Pholidota). Zool Stud 46, 389–396.
Xie, H.X., Liang, X.X., Chen, Z.Q., Li, W.M., Mi, C.R., Li, M., Wu, Z.J., Zhou, X.M., Du, W.G., and Harris, K. (2022). Ancient demographics determine the effectiveness of genetic purging in endangered lizards. Mol Biol Evol 39, msab359.
Yang, Y., Lin, Y., Wu, J., and Hui, C. (1994). Variation in mitochondrial DNA and population structure of the Taipei treefrog *Rhacophorus taipeianus* in Taiwan. Mol Ecol 3, 219–228.
Zang, Z.H. (1998). Overview of archaeological research in Taiwan (in Chinese). Relics Museol 4, 53–61.
Zhang, C., Dong, S.S., Xu, J.Y., He, W.M., Yang, T.L., and Schwartz, R. (2019). PopLDdecay: a fast and effective tool for linkage disequilibrium decay analysis based on variant call format files. Bioinformatics 35, 1786–1788.
Zhang, F., Wu, S., Zou, C., Wang, Q., Li, S., and Sun, R. (2016). A note on captive breeding and reproductive parameters of the Chinese pangolin, *Manis pentadactyla* Linnaeus, 1758. ZooKeys 19, 129–144.
Zhu, G., and Qiao, H. (2016). Effect of the Maxent model's complexity on the prediction of species potential distributions. Biodivers Sci 24, 1189–1196.